

QUANTIFYING VEGETATION RECOVERY ON SANTA ROSA ISLAND

A Thesis

by

ELIZABETH MARY RENTSCHLAR

Submitted to the Office of Graduate and Professional Studies of  
Texas A&M University  
in partial fulfillment of the requirements for the degree of

MASTER OF SCIENCE

Chair of Committee,	Chris Houser
Committee Members,	David Cairns
	Rusty Feagin
Head of Department,	David Cairns

December 2014

Major Subject: Geography

Copyright 2014 Elizabeth Mary Rentschlar

## ABSTRACT

The rate of recovery on barrier islands after hurricanes is not well understood, because the majority of studies have focused on the geomorphic impact of storms on barrier islands. Dune vegetation recovery is a vital component of barrier island recovery because it promotes the deposition of the sand required for dune stabilization. Despite a paucity of studies that quantitatively characterize vegetation recovery following hurricanes, Escambia County, Florida, was advised to spend nearly half a million dollars on revegetation efforts following relatively minor damage during the 1998 hurricane cycle. This research seeks to better understand that process by quantifying changes in vegetation extent between 1994 and 2010 on Santa Rosa Island, Florida following Hurricanes Opal and Ivan. Multispectral airborne imagery is used to analyze vegetation patterns and recovery. If no vegetation is present, sediment will not be deposited consistently. The clumps of plants collect sand in their wind shadows that grow and merge to create dunes. Changing patterns of vegetation distribution over time are examined in a geographic information system. The Verhulst logistic growth model is used to describe post-hurricane vegetation recovery. The logistic growth models results indicate that given twenty-five years of observed data, vegetation recovery occurs in approximately ten years on the Fort Pickens portion of the island and after fifteen years on the Santa Rosa Island portion of the island. The Verhulst model reveals that vegetation growth rates ( $r$ ) are higher in the overwashed transects. This is most likely the result of variations in the plant species found in an overwashed transect. The

transects in which vegetation spread to a greater portion of the transect (K) were more commonly collision dominated. This was probably because greater portions of these transects were less vulnerable to disturbance from run-up. Results suggest that there is a time lag between beach recovery and dune recovery that can be explained by vegetation recovery. This scale dependence will be affected by high-magnitude, high-frequency disturbances because it increases the chance that the vegetation will not have recovered before the next disturbance event thereby changing the dominant geomorphic regime. Fourier transformation reveals that there was an alongshore variation in the vegetation coverage before and after Hurricanes Opal and Ivan that corresponds to the frequencies of the ridge and swale bathymetry, around 1400 meters.

## TABLE OF CONTENTS

	Page
ABSTRACT.....	ii
TABLE OF CONTENTS.....	iv
LIST OF FIGURES.....	vi
LIST OF TABLES.....	viii
LIST OF EQUATIONS.....	ix
1. INTRODUCTION AND STUDY SITE DESCRIPTION.....	1
1.1 Introduction.....	1
1.2 Background.....	6
1.2.1 Barrier Island Response to Storms.....	6
1.2.2 Post-Storm Recovery.....	8
1.2.3 Vegetation Adaption Strategies.....	11
1.2.4 Vegetation Recovery.....	14
1.2.5 Population Models.....	16
1.3 Study Area.....	21
1.3.1 Santa Rosa Florida.....	21
1.3.2 Hurricanes.....	24
2. METHODS.....	27
2.1 Introduction .....	27
2.2 Data Acquisition and Preprocessing .....	27
2.3 Image Classification .....	29
2.3.1 Decision Tree .....	32
2.3.2 Support Vector Machine .....	34
2.3.3 Object Oriented .....	36
2.3.4 ISODATA .....	38
2.3.5 Classification of All Imagery .....	40
2.4 Measure Vegetation Spatially along Santa Rosa .....	41
2.5 Spatial Frequency .....	43
2.6 Biogeomorphic Recovery Model .....	44
3. RESULTS.....	45

	Page
3.1 Study Area 1: Fort Pickens .....	45
3.1.1 Average Recovery .....	45
3.1.2 Geomorphic Regimes .....	47
3.2 Study Area 2: Santa Rosa Island .....	51
3.2.1 Average Recovery .....	51
3.2.2 Geomorphic Regimes.....	56
3.2.3 Spatial Frequencies.....	58
4. DISCUSSION .....	61
4.1 Implications of Changing Storm Frequencies .....	61
4.2 Implications of Changing Storm Magnitudes .....	65
4.3 Similarities and Differences of FP and SR .....	68
4.4 Implication for Future Works .....	71
5. CONCLUSIONS .....	72
REFERENCES.....	74

## LIST OF FIGURES

FIGURE	Page
1.1 Verhulst Population Growth Model .....	3
1.2 Impact of Variables on Verhulst Model .....	4
1.3 Definition Sketch of Sallenger Model .....	7
1.4 Impact of Overwash Frequencies .....	19
1.5 Impact of Surviving Population on Population Recovery .....	20
1.6 Hypothetical Vegetation Population .....	20
1.7 Study Site .....	23
2.1 Decision Tree Classification .....	32
2.2 Decision Tree Classification Results .....	33
2.3 Support Vector Machine Results .....	34
2.4 Object Oriented Results .....	37
2.5 ISODATA Results .....	38
2.6 GIS Model .....	43
3.1 Fort Pickens Average Recovery .....	46
3.2 Verhulst Model of Fort Pickens .....	46
3.3 Alongshore Variation in $r$ at Fort Pickens .....	48
3.4 Alongshore Variation in $K$ at Fort Pickens .....	48
3.5 Alongshore Variation in $r$ and $K$ at Fort Pickens .....	49
3.6 Alongshore Variation in Recovery Times at Fort Pickens .....	50
3.7 Santa Rosa Average Recovery .....	51

FIGURE	Page
3.8 Hurricanes Georges and Ivan as Time 0 in Verhulst Model .....	52
3.9 Hurricanes Opal and Ivan as Time 0 in Verhulst Model .....	52
3.10 Santa Rosa Transects 43 - 153 Averages Vegetation .....	54
3.11 Santa Rosa Verhulst Model Best Fit K .....	55
3.12 Santa Rosa Verhulst Model Pre Opal K .....	55
3.13 Santa Rosa Verhulst Model Pre Ivan K .....	56
3.14 Alongshore Variation in r and K at Santa Rosa .....	57
3.15 Alongshore Variation in Recovery Times at Santa Rosa .....	57
3.16 Alongshore Variation in r at Santa Rosa .....	58
3.17 Alongshore Variation in K at Santa Rosa .....	58
3.18 Fourier Transformation Peak Counts .....	59
3.19 Fourier Transformation Post Storm .....	60
3.20 Fourier Transformation Pre Storm .....	60
4.1 Recovery Time Series Based on Fort Pickens r and K .....	63
4.2 Recovery Time Series Based on Santa Rosa r and K .....	64
4.3 Recovery to Different Storm Intensities .....	66
4.4 Conceptual Model of Recovery Drivers .....	67
4.5 Vegetation Change between 1994 and 2010 .....	70

## LIST OF TABLES

TABLE	Page
2.1 Imagery Data .....	29
2.2 Accuracy Assessment of Decision Tree Classification .....	33
2.3 Accuracy Assessment of Support Vector Machine Classification .....	35
2.4 Accuracy Assessment of Object Oriented Classification .....	37
2.5 Accuracy Assessment of ISODATA Classification .....	39
2.6 Accuracy Assessment of All Classification .....	40
2.7 Accuracy Assessment for Years .....	41



## LIST OF EQUATIONS

EQUATION	Page
1 Run-up.....	6

# 1 INTRODUCTION AND STUDY SITE DESCRIPTION

## 1.1 Introduction

The frequency and intensity of hurricanes has been increasing since 1970 (Webster et al., 2005). The number of category 4 and 5 hurricanes has doubled globally and there is the potential for further changes in storm activity with a change in global climate (Webster et al., 2005). When a storm impacts a barrier island there are four dominant geomorphic responses to the disturbance; swash, where water levels during the storm do not reach the base of the dunes, collision, where the storm run-up scarp the base of the dunes and the beach, overwash, where the run-up penetrates the dune system taking sediment from the beach and dune system to the back of the island, and inundation, where the sea level rise submerges the island (Sallenger, 2000). The resiliency of a barrier island depends on the rate at which the foredunes can redevelop in both height and extent (Hesp, 2002). As the frequency of storm events increase, the threshold for collision and overwash disturbances are also decreased. Therefore an increase in storm activity may lead to catastrophic change in barrier island morphology and a loss of ecosystem function.

While there are a number of studies to characterize the way that storms alter beaches and dunes on the barrier island and how these features recover in the weeks and years following, there is a paucity of studies to quantify the rate and mechanisms of long-term recovery, and in particular vegetation recovery following storm events.

Vegetation disturbance and recovery studies have tended to focus on the impacts of human activities, such as off road vehicles and foot traffic, as well as impacts from grazing and sand mining (Brodhead and Godfrey, 1979, Perumal, 1994, Maun, 2009). Other studies of dune vegetation have focused on the stresses placed on plants by the coastal dune environment (Disraeli, 1984, Maun, 1998, Zhang and Maun, 1990). With increasing severity of weather events it is even more important to understand how the vegetation on barrier islands recovers so that future human efforts are more cost effective.

After a human disturbance, such as driving on the beach, vegetation can re-establish in 2 to 8 years, if the roots and rhizomes are not destroyed during the disturbance (Brodhead and Godfrey, 1979). Similarly, Snyder and Boss (2002) found three years after Hurricane Opal all of the vegetation recovery in dunes and sand flats was the result of seed banks or vegetation fragments that survived the storm. Population growth models have been used as population recovery models after high magnitude disturbances such as fires (Verhulst, 1838, Richards, 1959). The simplest of these models measures the growth rate of the population,  $r$ , to the carrying capacity of the environment,  $K$  (Figure 1.1). The  $K$  and  $r$  from these models have become shorthand for the way in which populations have adapted to handle environmental pressure. The  $r$  adapted species are early successional species that focus their resources into producing large numbers of seed and spreading quickly after a disturbance. While  $K$  adapted species put their energy into a couple of seeds that have a much higher chance of reaching adulthood. In terms of recovery, this means that the  $r$  adapted species can

recover quickly while the K adapted species take longer and must displace the r species. The difference in recovery time can lead the casual observer to believe that recovery has occurred when the r species have returned to the landscape but the K species have not.

The r and K population models are commonly sigmoid curves that define increasing growth up to a maximum population. These models are based on the observation that populations increase exponentially until they hit the carrying capacity of their environment at which time they become stable or decrease (Tsoularis and Wallace, 2002). In the case of dune vegetation, exposed sand is not available habitat because not all of it can support life. Sand is exposed in the swash zone where plants are unable to persist and other segments have too high salinity or have no soil moisture (Maun, 2009).

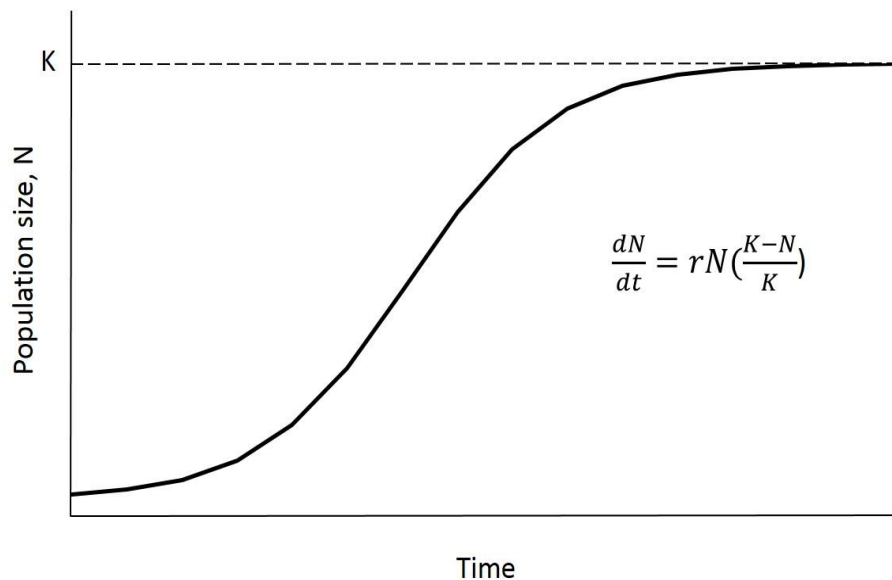


Figure 1.1 Verhulst Population Growth Model. The Verhulst (1838) population growth model has three inputs,  $r$ , the growth rate of the vegetation,  $k$ , the population limit of the vegetation, and  $N_0$ , the amount of vegetation immediately following the disturbance. The steepness of the slope is determined by the  $r$  value.

The exponential curves will only work for short term recovery but fail to account for the landscapes carrying capacity for the recovered vegetation population. If the carrying capacity is unknown the models can be used to determine the growth rate and the carrying capacity if the population size is known for different points in time, or if the carrying capacity is known and there is a single known population in time the growth rate can be estimated using the model (Figure 1.2).

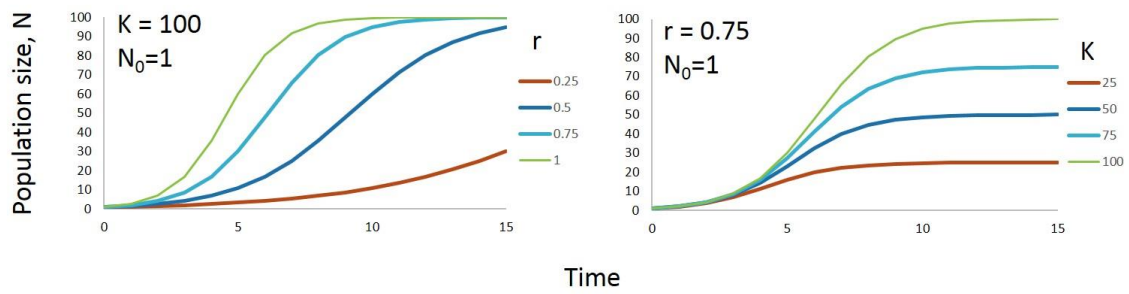


Figure 1.2 Impact of Variables on Verhulst Model. The left shows the variation in curves based on a changing growth rate ( $r$ ), on the right the changes that occur to the curves is shown with a changing carrying capacity. The amount of time for recovery changes if the growth rate changes, but the amount of time needed for recovery with different  $K$  values is consistent.

This thesis quantifies the vegetation extent on Santa Rosa Island in Northwest Florida before and after Hurricane Ivan (2004) in order to determine spatial variability of recovery rates in relation to the morphologic and the geologic framework. The objectives were to:

- Quantify vegetation extent along Santa Rosa from before Hurricane Opal to 2010 at regular intervals alongshore and model the data with the vegetation recovery model.
- Quantify spatial variance of vegetation extents and recovery alongshore.
- Relate the vegetation recovery to storm frequency.

If the frequency of overwash increases the current vegetation communities will not be able to recover to their carrying capacity before the next overwash event.

## 1.2 Background

### 1.2.1 Barrier Island Response to Storms

Sallenger (2000) created a geomorphic regime model that explains the relationship between the impact of a tropical storm and the ratio of the run-up and foredune heights. The controlling process regimes are broken down to the swash, collision, overwash, and inundation. In the swash regime, run-up does not reach the base of the dunes ( $R_{\text{high}} < D_{\text{low}}$ ) and erodes the beach face which will then be re-deposited after the storm (Figure 1.3). Stockdon et al. (2006) calculates run-up with two parameters, setup and swash (Equation 1).

$$R_2 = 1.1 \left( 0.35\beta [H_o L_o]^{\frac{1}{2}} + \frac{[H_o L_o (0.56\beta^2 + 0.004)]^{\frac{1}{2}}}{2} \right) \quad (1)$$

where

$H_o$  is the deep water wave height

$L_o$  is the deep water wavelength

$\beta$  is the angle of the beach slope

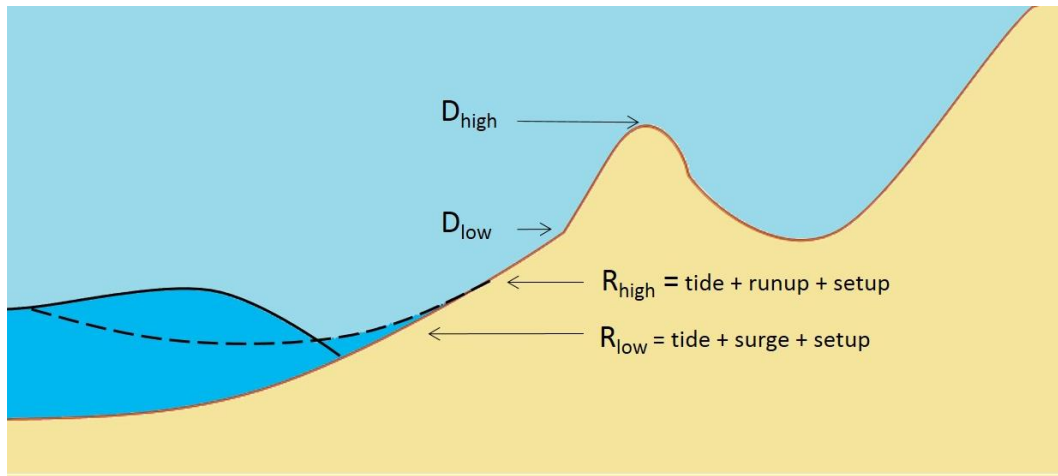


Figure 1.3 Definition Sketch of Sallenger Model. Definition sketch showing  $R_{high}$ ,  $R_{low}$ ,  $D_{high}$  and  $D_{low}$ . The dashed lines represent the swash excursion about wave setup (solid line). Figure adapted from Sallenger (2000).

During the collision regime, the height of the run-up relative to the beach face is great enough that the surge waters reach the base of the dune and scarping of the foredunes occurs which results in net erosion of the island dune system ( $D_{low} < R_{high} < D_{high}$ ). Most of the vegetation on the island survives these disturbances which only impact any vegetation that is growing at the base of the dune toward the beach.

The overwash regime occurs when the run-up heights are greater than the heights of the dunes ( $R_{high} > D_{high}$ ), this leads to the transportation of sediment from the dunes into the lagoon side of the island (Sallenger, 2000). When the surges to foredune ratio are greatest, inundation overwash occurs, the surge level is high enough for the overwash to penetrate the backshore dunes and reach the back side of the island ( $R_{low} > D_{high}$ ) (Sallenger, 2000, McCall et al., 2010). Vegetation works to slow the speed of the water which decreases the amount of sand that makes it to the lagoon, but much of the vegetation itself is buried or washed away. The movement of sediment to the back of the island causes the island to retreat toward the mainland. As long as the dunes are able to



reestablish this keeps the island from drowning when sea levels rises, but is destructive to human infrastructure and vegetation on the island. Parts of the island that are narrower and have smaller dunes have a greater risk of washover occurring (Sallenger, 2000). In contrast, portions of the island where the dunes are higher and wider experience washover less frequently. On occasions when waves do break through the foredune, the deposition tends to occur in the same location overwash has occurred in the past (Davidson-Arnott, 2010).

### 1.2.2 Post-Storm Recovery

The ability of a barrier island to withstand the next storm is dependent on the ability of the dunes to recover in height and extent before the next storm. Island recovery has been described in term of four stages: beach recovery, back beach recovery, dune formation, and vegetation recolonization (Morton et al., 1994). Beach recovery occurs quickly because the sand that was removed from the island during the storm is moved out into the near ocean where it is stored in the bars. The sand in the upper shoreface and the bars then accrete within as little time as a year, as Leadon (1999) observed after Hurricane Opal hit the Florida panhandle. It is during this initial stage of recovery when the island is the most vulnerable to disturbances because this is when the angle of the beach slope is the shallowest which allows for more run-up. The back beach begins to increase in elevation as the beach is restored; wind and water carry the sand from the beach to the back beach. This stage has been observed to begin during the second summer following the initial disturbance (Morton et al., 1994). The buildup of the back beach increases the beach slope which slows or prevents run-up from reaching

the base of dunes. The third and fourth stages of recovery are difficult to differentiate temporally due to their interdependence. Morton et al. (1994) defines the third stage as the dune formation and the fourth stage as the vegetation recolonization. Vegetation recolonization is necessary for the stability of the growing dunes (Morton et al., 1994). If no vegetation is present, sediment will not be deposited consistently. The clumps of plants collect sand in their wind shadows that grow and merge to create dunes. As dunes grow the amount of setup needed to push run-up to the height of the dunes continues to increase which decreases the odds of overwash events occurring.

Duran and Moore's (2013) dune recovery model focuses on Morton et al. (1994)'s third and fourth stages by simplify recovery down into quantifiable interactions between sand transports relation to vegetation and vegetation and the shoreline. Morton et al. (1994) attributes the rate of dune and back beach vegetation recovery to the amount of vegetation present before the storm and the amount of vegetation that the storm removes. Duran and Moore's (2013) model used vegetation as a roughness element to determine the rate at which sand deposition would be occurring. They also incorporated the age of the vegetation as a control for the vegetation's height. This was important because the height of incipient dunes is positively related to the height of the plant species that colonize it, while the length of the dune is negatively related the height of the plants. Plant canopies that are low-lying slow wind velocities less than taller plants. Where Duran and Moore's (2013) model falls short is the exclusion of plant species that do not grow upward in height. These stabilizing species instead spread vertically along

the sand and require dense vegetation growth to slow the wind to a speed that sand deposition will occur, where tall species do not have to be as dense (Hesp, 2013).

The development of dunes in the overwash throat, prevent future overwash on top of the current overwash fan, allowing for vegetation to recover on the rest of the feature (Matias et al., 2008). Stallins and Parker (2003) found that the species of plants that were highly abundant in historically overwashed sections were adapted well for recolonization of disturbed areas because these species had a higher likelihood of spreading through rhizomes. They found that the species composition on an overwash fan to be highly homogenous as a result of the colonizing species ability to spread quickly. The creeping behavior of the plant species found growing on the overwash decreased their effectiveness as dune builders but increased their ability to stabilize sand. Recolonization by dune building species such as *Croton punctatus* require long periods of time for plants to produce seeds, for those seeds to germinate, and for the new seedlings to grow to a size capable of capturing significant quantities of sand. Vegetation distribution and sediment size are ultimately what lead to the healing of the washover, although, no healing can occur if the storm frequency is higher than recovery time of vegetation (Hosier and Cleary, 1977).

Wolner et al. (2013) proposed that the frequency of disturbance controls which vegetation types are able to propagate on an island, this creates a positive feedback between plant species and geomorphic control regimes. On an island that experiences many disturbances the washovers will be recolonized by maintainer species, these are r adapted species. This is occurring because recovery to pre storm plant communities

does not have time to occur and the community composition changes as a result of increased disturbance activity. The more the disturbances occur the greater the proportion of the maintainer species will be, therefore the lower the dunes will be and the more likely that the island will be disturbed again. On the other hand, the island that receives a few infrequent disturbances will slowly increase in the number of dune building species. These species have more of a K adaption strategy than the maintainer species. These species alter their landscape to be more suitable habitat by building the dunes around them. The larger the dunes, the less likely overwash will occur and the greater chance that the dune building species will have at being the dominant plant group.

### 1.2.3 Vegetation Adaptation Strategies

The vegetation on dunes is classified into three categories, dune builders, burial-tolerant stabilizers, and burial intolerant stabilizers (Miller et al., 2010). The plant communities found in different geomorphic control regimes of the barrier islands are dependent on the individual plants response and adaptations to stresses placed on plants by the coastal dune environment (Zhang and Mauns, 1990, Zhang and Mauns, 1992, Ayyad, 1973, Boyce, 1954, Maun, 1996, Klimes et al., 1993, Amsberry et al., 2000). Stallins and Parker (2003) located dune builders on the dunes, burial-tolerant stabilizers in areas that are prone to overwash, and burial intolerant stabilizers in the interdunes where they were protected from overwash. Similarly Feagin and Wu (2007) identified a strong spatial distribution of plants functions along elevation gradients. The colonizing species (burial-tolerant stabilizers) were common in the low elevations, the competitor

species (dune builders), which were never found in close proximity to the colonizers, were found at the higher elevations on the developed dunes.

The plant communities along a dune system vary depending on the amount of sand that is accreted due to the variations in plants abilities to respond to burial events (Perumal, 1994). This is because plants respond differently to gradual burial and sudden burial events. Studies such as Maun (1996) incorporated burial timing by exposing seedlings to burial events at 8 day intervals. The seedling responded more to the stimulation of many small burials than during a single burial performed by Zhang and Maun (1990). Adult plants respond similarly to burial as seedlings, but their greater energy reserves mean that they are able to withstand more onerous conditions than the younger plants. Different plant species are able to emerge from a burial event at different rates. The faster they are able to emerge the greater their chance of retaining their viability (Maun, 2009). Baas and Nield (2007) successfully integrated the levels of burial tolerance of three species into their model of dune development in vegetated landscapes. By doing so they were able to repurpose a model of dune development in a vegetation free area for use in a coastal environment and show that it is possible to describe the impact of vegetation on a coastal landscape empirically. This demonstrated that variations in the vegetation's annual growth rate, response to burial and erosion have on the type of dune system that develop in a landscape and that by only modeling vegetation as grass is misrepresenting the complex relationship between dune and vegetation growth.

Burial-tolerant stabilizers need to be well adapted to salt exposure, but unlike the dune builders they need to respond well to large burial events. These species are well adapted to quickly colonizing the exposed sand of overwash terraces by creeping low to the ground. This means that burial-tolerant stabilizers are often the first vegetation types to recover to their pre-storm extents. Dune builder species need to be well adapted to salt exposure and small burials as they are the most exposed to ocean spray and receive the sand that is being blown up from the beach. The very adaptations that lead dune builders to be efficient at slowing sand increase the amount of time that it takes for the species to spread in the environment because they expend their resources into growing up ward. The burial intolerant stabilizers are protected from the brunt of the sea spray and from most burial events.

For plants to survive in a coastal environment they must find nutrition in a nutrient deficient environment and survive high exposure to salt. Salt spray from the ocean contains all of the nutrients that plants need to grow, but this spray also contains larger concentrations of salt that may stress the vegetation. The best scenario for vegetation health is when there is rain to wash the salt off the plants and leach through the sand where it is able to provide nutrition to the roots. When there has not been rain the salinity of the sand is greatest at the surface, rain does not result in higher salinity levels throughout the sand because it washes it to the water table (Ayyad, 1973). In studies where salt spray was applied daily, the younger leaves exhibited damage more quickly than the older leaves. The damage occurs first at the tips and spreads along the edges that then spread inward until the leaves die (Boyce, 1954). Coastal dune species

have developed a variety of tolerance and avoidance strategies for salt: leaves that receive higher amounts of salt become thicker (Boyce, 1954), some species only grow in portions of the island that are elevated or back from the ocean where they are less exposed to salt spray (Randall, 1970), other species have developed a mechanism that allows them to secrete excess salt from their leaves or roots (Maze and Whalley, 1992).

#### 1.2.4 Vegetation Recovery Studies

Vegetation disturbance and recovery studies tend to focus on the impacts of human activities which are seasonal or onetime events. Beach driving is a relatively common seasonal disturbance, Brodhead and Godfrey (1979) study of Cape Cod found that after 70 - 175 passes by vehicles the vegetation was completely eliminated. The roots and rhizomes that were not destroyed took 2 to 8 years to grow into plants of the same biomass as the control group. A more extreme single disturbance affecting vegetation on some beaches is sand mining, which completely removes the plant and the root system from the mined location. Partridge (1992) found that vegetation had not returned to a pre-mined community 40 years after the disturbance. There was new vegetation, but it was more homogenous than the control areas, the dominant plant species was an early successional species that prevented the introduction of other plants.

Few studies have analyzed the long term recovery of dune vegetation after hurricanes. Hurricanes are quite different from human disturbances in that the frequency of events is dependent on climactic conditions, not government policy. Miller et al. (2010) and Snyder and Boss (2002) examined the short term, less than 3 years, recovery of vegetation on barrier islands after storm events. Miller et al. (2010) considered 3–5

year period of vegetation recovery to its pre-storm extent but did not actually measure this rate of recovery. This does not fit with the findings of Stone et al. (2004), who claimed that the island did not even begin to recover until 6 years following Hurricane Opal. The major reason for this variation in recovery rates comes from the locations that the two studies were performed, despite being on the same island the two studies were performed in locations dominated by different geomorphic controls. Snyder and Boss (2002) found that after three years all of the vegetation recovery in dunes and sand flats could be attributed to seed banks or vegetation fragments, and not to plants spreading or new seeds. Miller et al. (2010) and Snyder and Boss (2002) both used grids to take vegetation censuses, Miller et al. (2010) was over nine years where Snyder and Boss (2002) was only three years after a hurricane event. Snyder and Boss (2002) did not have vegetation data before Hurricane Opal, so they used a similar island as a proxy for the vegetation on Santa Rosa before the storm. The focus of their paper was not on the quantity of vegetation, but instead on the biodiversity of the vegetation present.

Gornish and Miller (2010) used the nine year data set that Miller et al. (2010) collected on Saint George island to build models of vegetation response to storm frequency over 100 years. The model focused on the occurrences of individual species, finding that the foredunes declined in biodiversity and in total number of plants present when the frequency of storms increased. When coupled with Stallins and Parker (2003) findings that segments of the island with lower plant diversity were the same segments that were experiencing repeated overwash the implication would be that the island being studied in Miller et al. (2010) will not recover to its pre storm dunes. In Gornish and



Miller et al. (2010) model backdune areas were less affected by increased rates of storms. This may be due to the model failing to incorporate the geomorphic controls on the island, such as overwash, which have a high potential to disrupt the backdune.

#### 1.2.5 Population Models

Hugenholtz and Wolfe (2005b) incorporated a logistic model of vegetation growth into their model of dune stability based on the area of vegetation present in the dune field (Figure 1.1). This study will use a logistic model in a similar way, by applying it to vegetation as a whole and not splitting out the individual species. It is possible to undertake recovery studies of barrier islands following multiple storm events using remote sensing data that would not be possible to study using field work, but the nature of the publicly available imagery limits the ability to determine individual plant species.

Population models have been developed to explain the presence of different plants over time following a disturbance (Hugenholtz and Wolfe, 2005a). The coastal environment is a successional environment that exhibits similar vegetation recovery patterns as fire scarred lands, landslides, and areas following a flood. These are all secondary succession where the land is not entirely devoid of life like a lava flow. Succession occurs when the first species is introduced to the nearly barren land, this step is often not necessary if some of the plant species survived the disturbance. The species will then colonize the area and eventually reach a stage of naturalization. The first plant species that grow in the environment are r adapted species that focus their resources on producing large numbers of offspring quickly. After some time has passed the k adapted

species are introduced and slowly begin to colonize. These plants focus on a smaller number of offspring than the  $r$  adapted species, so the individuals take a longer time to grow and reproduce.

The population models that are used are intended for only one species at a time. This has meant that many of the modern models are more complex than the Verhulst (1838) model as they also account for the  $r$  adapted species decline following the introduction of the more  $k$  adapted species. The focus of this study is not on the biodiversity of the plant species on the island, although biodiversity is an important area for future studies. From a geomorphic perspective the recovery of the vegetation as a community is more important than the recovery of any one individual species.

The Verhulst (1838) population growth model has been a foundation piece in the way that modern science understands population behavior. The model requires three inputs,  $r$  which is the growth rate of the vegetation,  $k$  which is the population limit of the vegetation, and  $N_0$  which is the amount of vegetation immediately following the disturbance. The study will be the first to use the Verhulst model to characterize the rates of vegetation recovery on a barrier island following a hurricane or tropical storm. This will make it possible for future studies to model recovery in similar environments with less vegetation data than was used in this study.

Before any data is analyzed with the model it suggests that with the increasing frequency of overwash in coastal areas the time necessary for recovery to occur may not pass before the next overwash occurs (Figure 1.4). But not every storm that hits the island cause the same level as damage because the beach slope changes with time and

the setup varies with the force of the storm and with the segment of the beaches relationship to the ridge and swale bathymetry. The amount of vegetation that survives a storm has a large impact on the amount of time it will take the plant population to recovery (Figure 1.5). When the dunes and plant population are well established on the island minor storms will have little impact on the plant population, but following a major storm, minor storms can set the recovery process back years. In the case of increasing overwash frequency where the vegetation is not able to return to near carrying capacity the plant communities would change to species that are r adapted, this would allow for quicker spreading of the vegetation but would also result in fewer dune building species thereby decreasing the size and extent of the fore dunes (Figure 1.6).

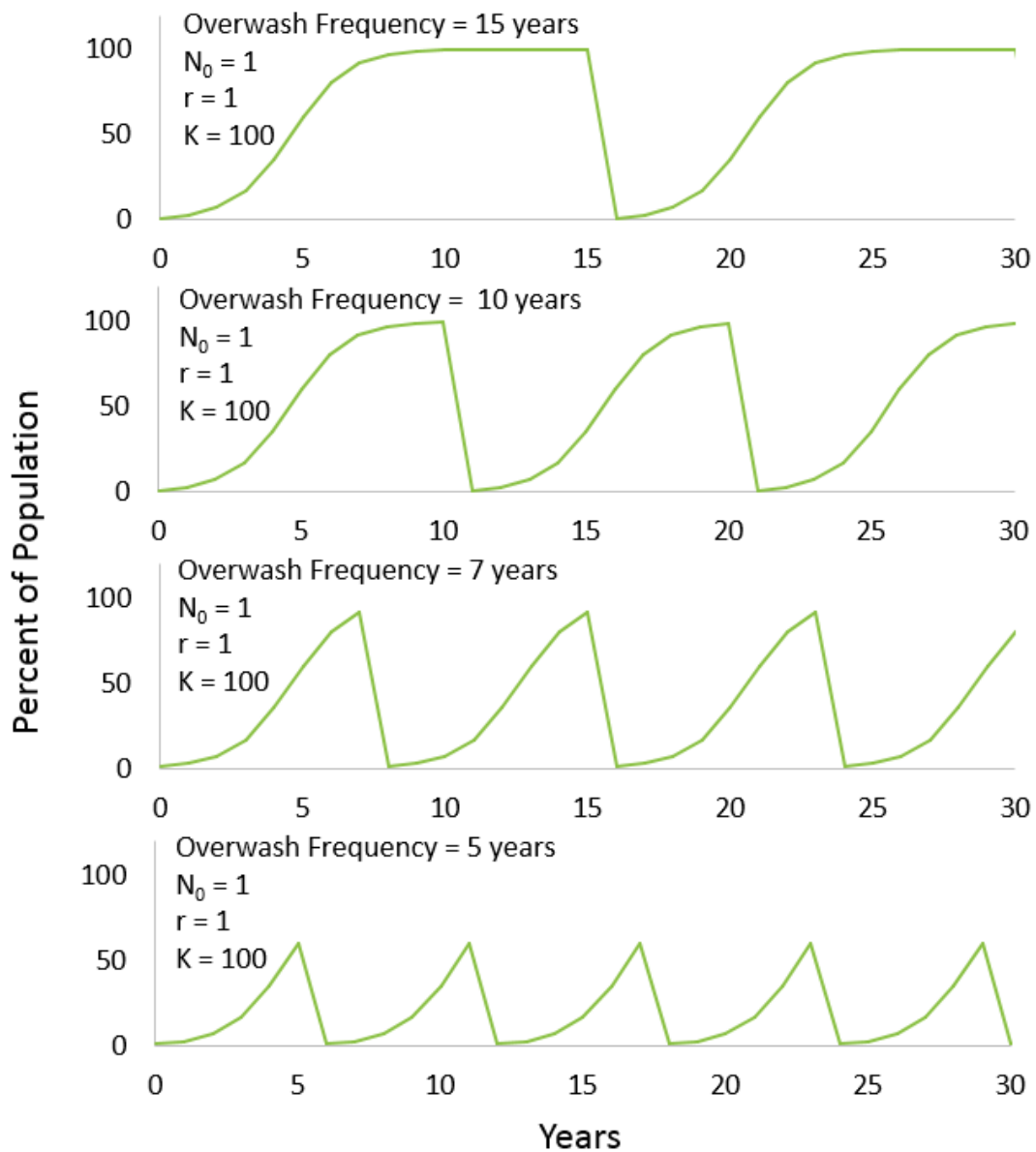


Figure 1.4 Impact of Overwash Frequencies. The ability of the population to recover is dependent on the frequency at which disturbances occur. The figure compares the recovery of a population that returns to 1% of the population capacity after each overwash disturbance. For this example the growth rate of 1 means that the population more than doubles from one year to the next until it approaches the upper limit. As the number of disturbances increase the population is less and less able to recover. If less than 1% of the population capacity survived after each disturbance the population would take an even greater amount of time to return to its pre storm condition.

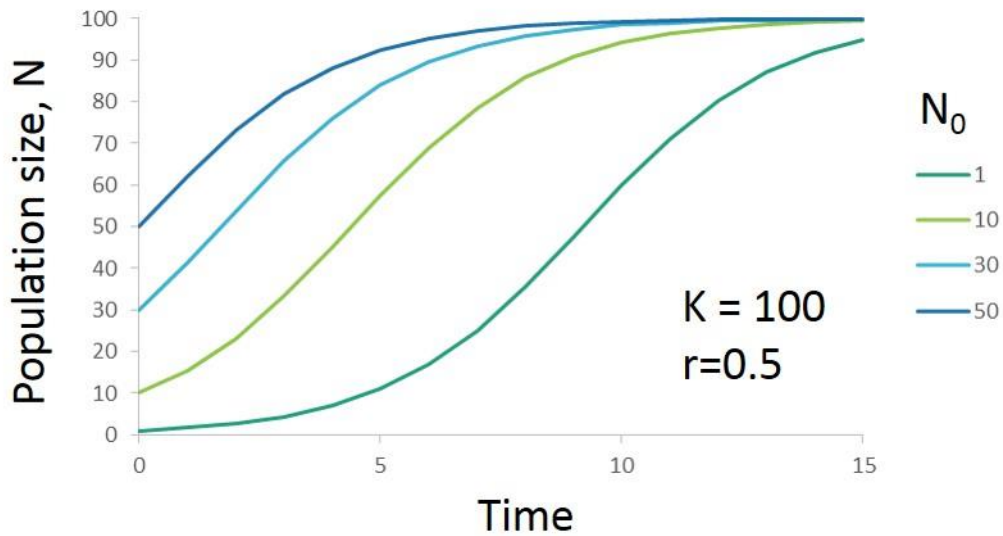


Figure 1.5 Impact of Surviving Population on Population Recovery. The amount of time that a population takes to recover is impacted by the amount of damage that occurred to the initial population.

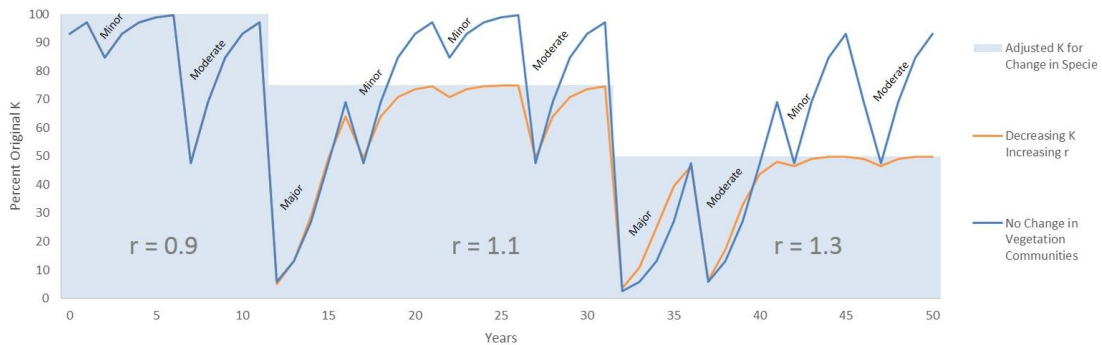


Figure 1.6 Hypothetical Vegetation Population. The time series shows a hypothetical vegetation population on an island that experiences storms of varying intensity around a 5 year interval. The blue line represents the vegetation recovery if the vegetation community remained constant throughout the time. The orange line represents the vegetation recovery if the vegetation community has a shrinking carrying capacity,  $K$ , and an increasing growth rate ( $r$ ). Assumed that the damage would be consistent for the two plant communities.

### 1.3 Study Area

#### 1.3.1 Santa Rosa Florida

Santa Rosa Island is the second longest barrier island on the Gulf coast, following only Padre Island. It is located in the Florida panhandle near the city of Pensacola, with a length of 95 km. The island has an average width of 500 m, although it ranges from 150 to 1000 m. The coastal shelf has a relatively a low-gradient and the waves are typically low-energy. The island is almost entirely made up of 100% quartz sand with an average diameter of 0.25mm (Miller et al., 2001). The sediments making up the island comes from the longshore distribution of the eroded remnant of a Pleistocene core (Otvost, 1982, Stone et al., 1992). The island subsequently transgressed landward to create ridge and swale topography (Houser, 2012). The sediment budget of Santa Rosa is balanced with around 50,000 m<sup>3</sup> a year coming to the island and 47,000 m<sup>3</sup> a year being transported offshore (Stone and Stapor, 1996).

Offshore of the island are sinusoidal ridges and troughs oriented northwest-southeast (Stone et al., 1992). The largest foredunes are found to the west of cusped headlands, the wider sections of the island. The widest sections of the island corresponded with the locations of the large ridges but the dunes landward of the transverse ridges are limited in their supply of sediment. These ridges then provide sediment to the littoral budget which deposits the sediment to the west of the ridge but these same dunes that are landward of the swales are limited in the ability of sediment to be transport to the dunes (Houser and Hamilton, 2009). The swales have reflective to intermediate nearshore profile which have more destructive run-up leading to a greater

probability of overwash occurring in these locations and are predominantly smaller discontinuous dunes. The ridges have intermediate to dissipative near shore profiles which discourages the large run up in these locations increasing the chances that they will experience swash or collision and have larger more continuous dunes. Houser et al. (2008) used spectral analysis to relate the spatial variation in dune morphology, offshore bathymetry, shoreline change, and island width on Santa Rosa Island. They found that there was a statistical correspondence at length scales 750, 1450, and 4550 meters.

Historically the shoreline of Santa Rosa Island has been stable with only a 0.1 m per year retreat toward the mainland (Morton et al., 2004). The frequency of cyclone events in the area has increased since 1995 (Stone et al., 2004). Prior to Opal in 1995 the last major storm had been Hurricane Frederic in 1979. In the 15 years following Opal there have been four large storms to impact the island. This has led the once stable shoreline to become one with great shoreline transitions during the Hurricanes Opal and Ivan, because storms are a significant factor in shoreline migration through overwash events (Morton et al., 1995). Following the 2004 and 2005 hurricane season Houser and Hamilton (2009) observed the SR study site shift from a landscape dominated by continuous dunes and hummocky back barrier dunes to one dominated by washover terraces and washover corridors.

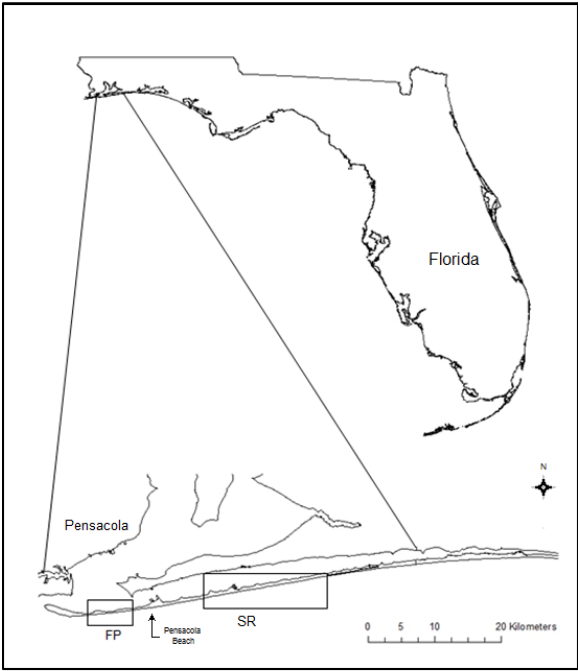


Figure 1.7 Study Site. The map shows the location of the Fort Pickens (FP) section of the island and the Santa Rosa (SR) section of the island.



### 1.3.2 Hurricanes

Santa Rosa Island, Florida, is in a mild subtropical climate. The mean precipitation is 152 cm a year, with the highest amounts of rain occurring in the summer and late winter. From March to August the wind is predominantly from the south, but switch to strong northerly winds in the fall and weak northerly winds in the winter (Miller et al., 2001).

Hurricane Opal made landfall on Santa Rosa Island on October 4<sup>th</sup>, 1995. The hurricane was a category 3 and the strongest storm to have impacted the island in one hundred years (Stone et al., 2004). The nearshore waves reached heights of 8 m at least 4 times a minute. These waves removed foredunes that were less than 5 meters in height (Stone et al., 2004). In FP 70% of the sediment from the eroded foredunes was deposited along the back of the island by overwash (Stone et al., 2004). The back shoreline was pushed bay ward 40 m following the storm, although 20m were eroded in the 2 years following the storm (Stone et al., 2004).

Shortly thereafter, Hurricane Danny made landfall on July 19<sup>th</sup>, 1997 off Mullet Point, Alabama, 70 km to the west of Santa Rosa Island. The hurricane was a category 1. The storm increased the amount of sediment delivered by the near shore current. Strong southerly winds increased dune volume with a deposition rate of 0.2 m<sup>3</sup> (Stone et al. 2004). A little over a year later Hurricane George made landfall early in the morning of September 28<sup>th</sup>, 1998 in Biloxi Mississippi, 160 km to the west of Santa Rosa Island. The cyclone was a strong category 2. The slow movement of the storm increased the

amount of time that it impacted the coast. The nearshore waves reached heights of 10 m at least 4 times in a minute (Stone et al., 2004).

The island experienced a seven year reprieve before the next major storm impacted the island. Hurricane Ivan made landfall on the 16<sup>th</sup> of September, 2004 in Alabama 45 kilometers to the west of the Santa Rosa Island. At the time of landfall, Ivan was a category 3 hurricane with wind forces extending 170 km from the eye (McCall et al., 2010). The entire island experienced the wave and surge activity that occurs within the extent of the hurricane force winds (Claudino-Sales et al., 2008). The National Data Buoy Center measured waves between 16 and 12 meters offshore of the barrier island exceeding previous records (Claudino-Sales et al., 2008). The typical offshore wave heights in the area range between 1.2 and 0.8 m (Claudino-Sales et al., 2010). The measurements of the surge above mean lower low water were limited by the capacity of the Pensacola tide gauge, which recorded the highest surge at 2.1m, although it is believed that they were higher (Claudino-Sales et al., 2010). For a period of ten hours, the surge level was 1.5 meters above mean lower low water (Claudino-Sales et al., 2010). These measurements of the surge do not include swash run-up along the beach or the wave setup (Claudino-Sales et al., 2010). Houser et al. (2008) found that Hurricane Ivan resulted in a  $-38.0 \pm 2.1$  m/yr minimum movement across the entire island toward Florida's main land and a maximum erosion rate of  $-54.4 \pm 2.1$  m/yr.

Less than one year after Hurricane Ivan made landfall, Hurricane Dennis struck land near Pensacola on July 10th, 2005. Dennis was a category 3 storm with wind forces of 51-53 m/s. The shore line of the Santa Rosa study area retreated around 57 m and the

2.8 m foredunes were overwashed leaving a steep foreshore and washover sheets. In the year following the beach erosion 19 m were redeposited on the beach (Houser and Hamilton, 2009). Houser and Hamilton (2009) found that the along shore recovery of the island following the 2004 and 2005 hurricane season was related to the island width, the transverse ridges on the inner shelf, the height of the pre-storm dunes, and the extent of the overwash pinitrashion into the island.

## 2 METHODS

### 2.1 Introduction

Traditionally barrier island vegetation studies have been performed exclusively with field work, but collecting vegetation censuses is a time consuming and expensive approach because it requires multiple site visits over many years. Remote sensing provided an opportunity to use pre-storm imagery as a baseline from which dune vegetation recovery could be measured. This made it possible to perform recovery studies in locations that a storm event has taken place before the study was undertaken. Two undeveloped sections of the Santa Rosa Island were studied (Figure 1.7), the beach and dune recovery of these sites were studied in Houser and Hamilton (2009). The Fort Pickens (FP) section of the island is a narrow section of the island. Stone et al. (2004) study of short term impacts of hurricanes on barrier islands studied the same location. The Santa Rosa Island (SR) section of the island is a wider section of the island. The SR study area spans 15.5 km of the island.

### 2.2 Data Acquisition and Preprocessing

Images were acquired through the USGS earth Explorer, NOAA, Florida Department of transportation (FDOT) and from the National Agricultural Imagery Program (NAIP). 2010, 2007, 2004, 1999, and 1994 were downloaded with spatial information (Table 2.1). The 1997, 2000, and 2005 imagery were georeferenced. The 2007 orthorectified image was used as a base from which the 2005 images were

rectified. The 2004 orthorectified image was used as a base from which the 1997 and 2000 images were rectified. Using images that were between the same storms increases the chance that there were similar features that would be suitable as rectification points, such as maritime forest, lakes, buildings, and roads. The 2005 imagery was the most difficult to georeference because Ivan damaged the majority of the human infrastructure and removed many of the clumps of vegetation that made up the majority of co-registration references. The RMS errors obtained in other studies using aerial photographs range from 15m to 4m (Hughes et al., 2006). RMS errors that were similar or the same as these studies were consider acceptable. The average RMS errors were under 10.

After the images were co-registered, ENVI 4.8 was used to mask out the majority of the ocean, leaving only the island itself and a small border of water. This was done by creating a polygon Region of Interest (ROI), thereby allowing the study area to be extracted using the study area ROI. A mask value of -9999 was used to mask out the background. Masking out the water helped to expedite the classification process by decreasing the number and variety of pixel values.

Table 2.1 Imagery Data. The metadata of the imagery used and the dates of the major storms.

<b>Year</b>	<b>Source</b>	<b>Type</b>	<b>Resolution</b>
1994, Jan 31	USGS/NAPP	DOQ- 3.75- MIN CIR	1-meter
<b>Opal October 4 1995</b>			
1997, Feb 15	FDOT	B/W	0.33-meter
<b>Danny July 19 1997</b>			
<b>Georges September 28 1998</b>			
1999, Nov 27	USGS /NAPP	DOQ- 3.75- MIN CIR	1-meter
2000, Feb 15	FDOT	B/W	0.33-meter
2004, Jan	NAIP	DOQQ- CIR and visible	1-meter
<b>Ivan September 16 2004</b>			
<b>Dennis July10 2005</b>			
2005, July 12	NOAA	Aerial	0.33-meter
2007, Jan 9	NAIP	DOQQ	1-meter
2010, Jan 10	NAIP	DOQQ	1-meter

### 2.3 Image Classification

There were two elements to the first objective, first, to determine which classification method should be used, and second, to determine if classifications using only the visible bands could produce results that are as accurate as a classification based on visible and NIR for identifying vegetation in a coastal environment. This was done using NAIP imagery of the FP end of SR, FL in 2004 from before Hurricane Ivan in September of 2004. This was the only year for which the data has four spectral bands. Four classification methods were attempted to determine their viability for the project:

1. The **Decision Tree classifier** uses the knowledge of the user of the band values to create a classification. This is accomplished by a series of binary decisions or

nodes to place pixels into classes based on the RGB values (Safavian and Landgrebe, 1991).

2. **Support Vector Machine** (SVM) classification can provide accurate results even with small sample sizes as well as handle multi source data (Garcia et al. 2011). SVM is a non-parametric supervised classification method that is based on statistical learning. The algorithm separates the data into classes with hyperplanes based on the training data (Mountrakis et al., 2011).
3. **Object oriented classifiers** were developed to help overcome the problems of classifying high spatial resolution images (Cleve et al., 2008, Li et al., 2013). Higher resolution images are more likely to have a variety of spectral responses that represent the same object. When using traditional per-pixel classifiers, the high spectral variability increases the chance of salt and pepper classification noise. Object oriented overcomes this by incorporating the spatial relationship of pixels as well as the spectral relationship when determining the class an object (Myint et al., 2011).
4. **Iterative Self Organizing Data Analysis** (ISODATA) is an unsupervised classification method, meaning that it does not require user knowledge of the data prior to classification. It works by grouping spectrally similar pixels into classes which it then repeats (Cleve et al., 2008). The parameters were set so that the number of classes was between 5 and 20 with a maximum of 20 iterations and a change threshold of 5%. The classes were combined until there are only five or six left, water, tree, grass/shrub, road, sand, and unclassified. The road

and water class were then deleted and any visually identifiable corrections were made.

Before performing the object oriented classification, support vector machine, decision tree, or ISODATA classifications on the images the test regions of interest (ROI) were visually selected. The ROIs were used to perform the accuracy assessments that quantify which classification produced the best results. Fifty or more points were collected for the sand, road, water, tree, and grass/shrub classes. The pixels that are classified as the same classification in the ROI and the classified image are divided by the total number of ROI pixels to produce the overall accuracy. Each class has a producer's and a user's accuracy. The producer's accuracy is determined by dividing the pixels that were classified as water in the ROIs and in the classified image by all of the ROI pixels that were classified as water by the classification method. The user's accuracy instead divides the correctly classified pixels by the pixels identified in the ROI as that class (Jensen, 2005).



### 2.3.1 Decision Tree

To create the decision tree classification the pixels representative of the land cover classes were observed to determine the values where landcover classes varied from one land cover to another. This was time consuming. It requires the user to examine large numbers of pixels and a large amount of trial and error. The pixel divisions for the RGB bands and the RBG and NIR band images are almost the same, with the only difference being when the decision tree identifies water and non-tree vegetation (Figure 2.1). Water has a very low reflectance of NIR and Vegetation has a very high reflectance of NIR. The decision tree did not distinguish well between the water and road (Figure 2.2). The visible and NIR image performed better than the visible bands alone with an overall accuracy of 71% (Table 2.2).

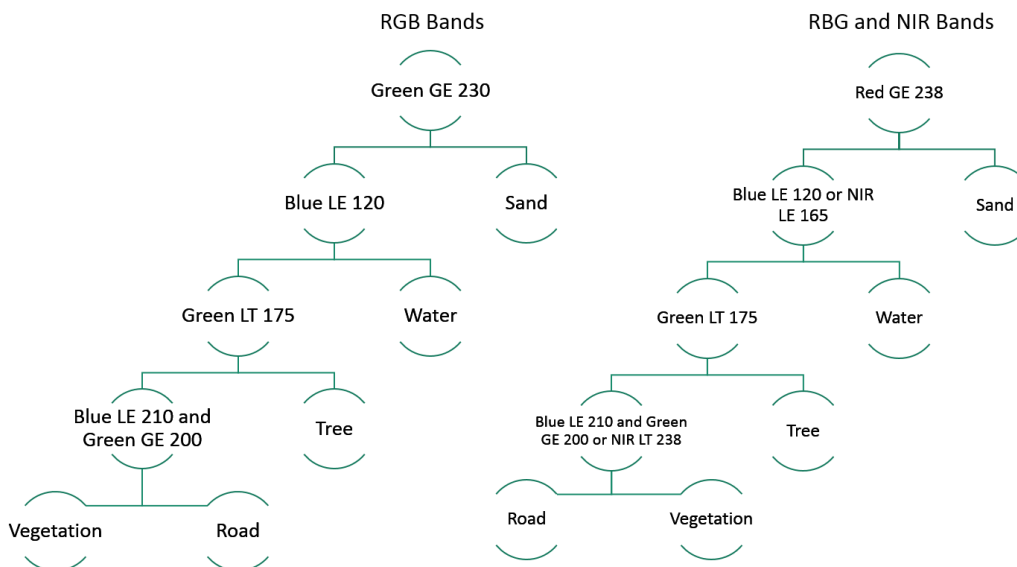


Figure 2.1 Decision Tree Classification. The decision tree used to classify the pixels in the RGB is on the left and the decision tree used to classify the RGB and NIR images is on the right. The nodes on the left side of the decision trees sort the pixels, if they do not meet the requirement then go to the class on the right

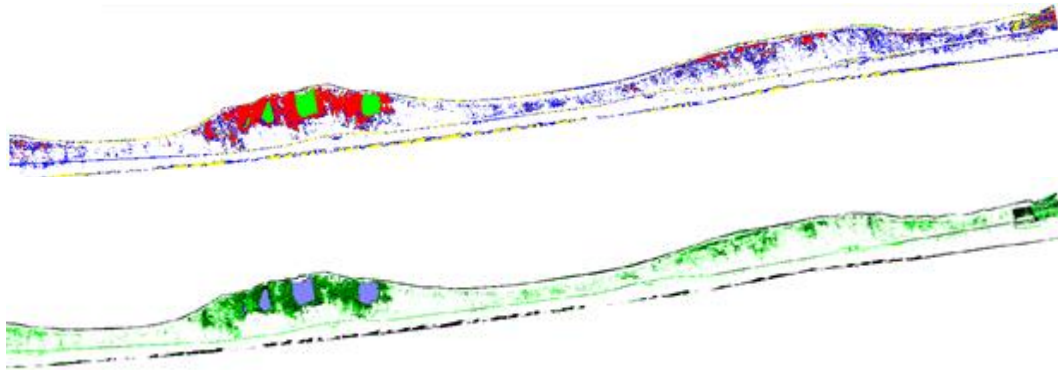


Figure 2.2 Decision Tree Classification Results. The classified images produced by the decision tree. The top image is of the RGB bands and the bottom image is of the RGB and NIR bands. In the RGB the red is tree and the blue is other vegetation. In the NIR the dark green is tree and the light green is other vegetation.

Table 2.2 Accuracy Assessment of Decision Tree Classification. The results of the accuracy assessment of the decision tree classification. Both images have low overall accuracies and Kappa Coefficients although they did well in classification of sand and trees.

	Visible Bands		Visible and NIR Bands	
Overall Accuracy	64%		71%	
Kappa Coefficient	0.55		0.58	
Class Accuracy	Producers Accuracy	Users Accuracy	Producers Accuracy	Users Accuracy
Water	28%	100%	90%	96%
Tree	97%	77%	95%	78%
Sand	100%	96%	100%	96%
Road	54%	45%	82%	65%
Other Vegetation	52%	42%	35%	63%

### 2.3.2 Support Vector Machine

To create the SVM classification training ROIs were collected in addition to the testing ROIs. For the training set of ROIs, 50 polygons were sampled for sand, road, water, and grass/shrub, however, only 40 polygons were collected for trees because of the limited number of trees in the images. In the creation of training ROIs, 0.5 meter CHM and 2004 image with RGB bands and NIR band were used to help find correct training data. The SVM classification method was then performed using a Radial Basis Function kernel type, the default gamma in the kernel function of 1.00, the penalty parameter of 100, and the classification probability thresholds of 0. The resulting classifications were quite similar (Figure 2.3). The Visible bands alone performed slightly better than the visible and NIR image with an 82% overall accuracy (Table 2.3).

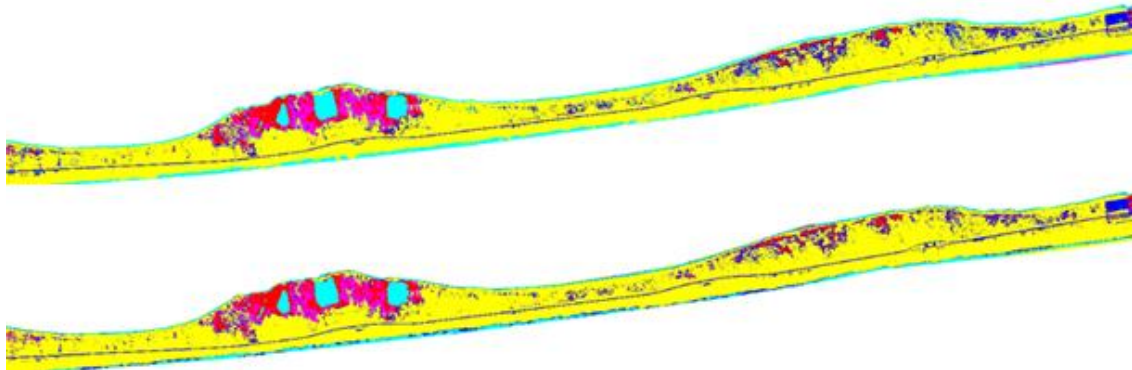


Figure 2.3 Support Vector Machine Results. The classified images produced by the SVM. The top image is of the RGB bands and the bottom image is of the RGB and NIR bands. In both images the red is tree and the fuchsia is other vegetation.

Table 2.3 Accuracy Assessment of Support Vector Machine Classification. The results of the accuracy assessment of the SVM classification. Both images did well in classification of sand and water.

	Visible Bands		Visible and NIR Bands	
Overall Accuracy	82%		80%	
Kappa Coefficient	0.77		0.75	
Class Accuracy	Producers Accuracy	Users Accuracy	Producers Accuracy	Users Accuracy
Water	98%	92%	96%	98%
Tree	92%	94%	86%	97%
Sand	100%	92%	100%	83%
Road	100%	65%	97%	66%
Other Vegetation	22%	86%	22%	70%

### 2.3.3 Object Oriented

The object oriented image segmentation and classification were performed using eCognition Developer 64. The image layer weights for the RGB bands were 1, 2, and 1. The image layer weights for the NIR and RGB were 3, 2, 1, 1. The green band and the NIR band respectively were given the largest weights in the two images because there are the most reflective of vegetation. Six classes were added into the class hierarchy for each image; empty (No Data), grass/shrub, road, sand, tree and water. Standard nearest neighbor feature space was defined by using mean and standard deviation. To train the classification 50 samples (objects) in each image were collected for each class throughout the two images. Two TTA mask was created for the selected samples from each image. The standard nearest neighbor classification was applied into all six classes. A visual assessment of the classified images shows that the visible bands classification over classified the non-tree vegetation (Figure 2.4). Despite this over classification of the vegetation the overall accuracy assessment of the visible object oriented was 90% (Table 2.4).

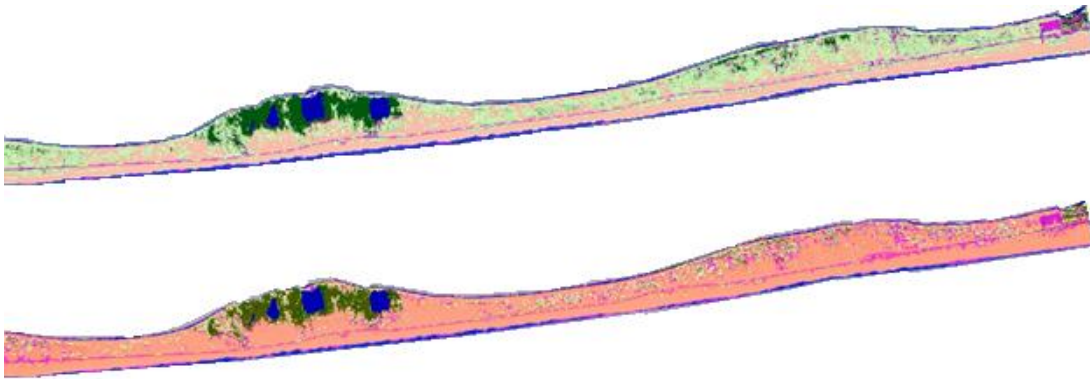


Figure 2.4 Object Oriented Results. The classified images produced by the object oriented method. The top image is of the RGB bands and the bottom image is of the RGB and NIR bands. The RGB image over classified the vegetation. In both images the dark green is tree and the light green is other vegetation.

Table 2.4 Accuracy Assessment of Object Oriented Classification. The results of the accuracy assessment of the object oriented classification. Both images did well in classification of sand and water.

	Visible Bands		Visible and NIR Bands	
Overall Accuracy	90%		88%	
Kappa Coefficient	0.87		0.85	
Class Accuracy	Producers Accuracy	Users Accuracy	Producers Accuracy	Users Accuracy
Water	100%	98%	96%	98%
Tree	89%	85%	84%	89%
Sand	90%	100%	100%	96%
Road	95%	87%	97%	80%
Other Vegetation	72%	78%	61%	80%

#### 2.3.4 ISODATA

The four layers in RGB and NIR and the 3 layers of RGB images were run through ISODATA. The number of classes were set between 5 and 20 with a maximum of 20 iterations and a change threshold of 5%. The resulting 4 layer classification had 20 classes and an unclassified class and the 3 layer classification had 11 classes and an unclassified class. The classes were combined until there were only five or six left, water, tree, grass/shrub, road, sand, and unclassified although the color classification did not differentiate between grass/shrub and road (Figure 2.5).

ISODATA is more time intensive on the back end of the classification. The only classes that were needed for the study was vegetation and sand. ISODATA did well in classifying vegetation and poorly with road and water which are the least important classes (Table 2.5). To correct for this the water was reclassified to vegetation (this was not done for road because there was none in the classification) and then converted the

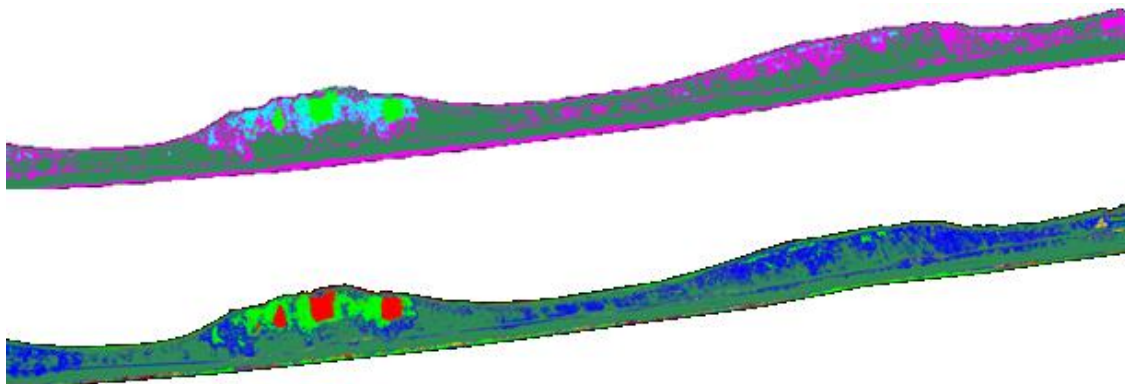


Figure 2.5 ISODATA Results. The classified images produced by the ISODATA method. The top image is of the RGB bands and the bottom image is of the RGB and NIR bands. The RGB image did not classify any road. In the RGB the blue is tree and the purple is other vegetation. In the NIR the green is tree and the blue is other vegetation.

Table 2.5 Accuracy Assessment of ISODATA Classification. The results of the accuracy assessment of the ISODATA classification. Both images did well in classification of sand and tree, and performed better on vegetation than the other classification methods despite having low overall accuracies.

	Visible Bands		Visible and NIR Bands	
Overall Accuracy	55%		64%	
Kappa Coefficient	0.47		0.56	
Class Accuracy	Producers Accuracy	Users Accuracy	Producers Accuracy	Users Accuracy
Water	25%	75%	32%	100%
Tree	78%	80%	95%	44%
Sand	100%	98%	100%	100%
Road	0%	0%	32%	84%
Other Vegetation	87%	31%	76%	48%

raster into a shapefile which allowed the water and the road to be deleted which was relatively simple as both land covers are bounded by sand and easily identifiable to the user. By removing the water polygons the misidentification (commission error) of vegetation was lessened. After removing these areas the accuracy assessment was re-performed based on three classes and had an overall accuracy of 94.7%, a Kappa Coefficient of 0.94, and a vegetation accuracy of 92.5%.

Contrary to expectations the highest uncorrected accuracy was the RGB object oriented classification (Table 2.6). This was closely followed by the SVM RGB classification, although the NIR object oriented performed better than the RGB only SVM classification.

These result show that it is possible to have accuracies as high, or higher than RGB and NIR using only RGB in a coastal environment. This validates the use of imagery with limited spectral information that was being used to measure the extent of vegetation in this study. The highest uncorrected accuracy was the object oriented



Table 2.6 Accuracy Assessment of All Classification. Compares the overall accuracies and that Kappa values of all the classified images produced by the four methods.

	Visible Bands		Visible and NIR Bands	
	Overall	Kappa	Overall	Kappa
Decision Tree	64%	0.55	71%	0.58
SVM	82%	0.77	80%	0.75
Object-Oriented	90%	0.87	88%	0.85
Isodata	55%	0.44	64%	0.56
Isodata - Corrected	95%	0.94		

classification using only RGB. It was possible though that this was displaying a bias created by the selection of the testing pixels. When selecting pixels it is natural for the user to select pixels that are in the middle of features. Object oriented classifications work to mimic the way the human eye can distinguish features by creating objects. This made it less likely that the testing pixels are located along the edges of classifications.

The corrected ISODATA classification had the highest overall accuracy. This was the classification method that was used for the rest of the first objective. This was not only because it had the highest accuracy but also because of the wide variety in the imagery that was used in the project.

### 2.3.5 Classification of All Imagery

The same input parameters that were used for ISODATA in the first half of the objective were used on all of the imagery. The accuracies were assessed using a confusion matrix after performing the classifications of all the imagery. The test pixels were selected new for each year and were based on a visual interpretation of the imagery. The Fort Pickens section of the island had 50 test pixels for trees, 80 for sand, and 80 for vegetation. The Santa Rosa Island section had 120 pixels for vegetation, 120

Table 2.7 Accuracy Assessment for Years. The table lists the overall accuracies, the Kappa values, and the vegetation class's accuracy by year.

Year	FP			SR		
	Overall	Kappa	Veg	Overall	Kappa	Veg
1994	99%	0.99	100%	99%	0.99	99%
1997	95%	0.95	89%	93%	0.92	87%
1999	98%	0.98	98%	95%	0.94	84%
2000	91%	0.91	84%	95%	0.94	88%
2004	95%	0.94	93%	95%	0.94	87%
2005	93%	0.93	82%	95%	0.94	86%
2007	91%	0.90	78%	94%	0.94	86%
2010	92%	0.91	81%	93%	0.92	88%

for sand, and 120 for marsh. There were not always enough vegetation patches in the images that were post hurricane to support the same number of test pixels in those years where recovery has occurred, so some years did not have as many test pixels as others. Jensen (2005) states that a Kappa that is greater than 0.80 represents strong agreement between the test points and the classified image. For this research the classifications that had a Kappa accuracy of 0.9 or better were accepted as these have a very strong agreement between the classification and the test pixels (Table 2.7).

#### 2.4 Measure Vegetation Spatially along Santa Rosa

In order to select and compare the vegetation extent on the same section of the island over multiple years, a transect system was established. The transects were built by drawing a polyline across the island that was edited with the COGO tool. This made it possible to segment the line into 100m sections. A copied parallel line was added 2 km away. Because both lines were separated into 100m pieces, it was possible to use their vertices as guide points in drawing rectangles that made up the transects. The

transects were each be 100m wide and 2km long. Most of the information in the long section of the transect was excluded because water was not of interest to this study.

A tool was created in model builder to extract the vegetation from the transects by using the iterate feature tool to select transects; each of which will then be used to clip my classification of sand, tree, and non-tree vegetation (Figure 2.6). Because vegetation may not be present in every transect over all of the years, the tool was designed to only use the transects with vegetation completely contained within the transect to prevent errors when the model attempts to determine the area of polygons in shapefiles that were empty. The tool determined the areas of the polygons, and then exported the data as ASCII files. By using %name% or %value% when naming the output features, they have unique names that will not be overwritten after each iteration. The areas of the vegetation polygons in the clipped layers were calculated after clipping to prevent double or triple counting of areas since the clipped polygons will retain all of their pre-clipped attributes. The size of each polygon was determined by adding a field to the attribute table representing the area in meters squared, which is easily calculated in ArcMap if all of the imagery was correctly projected and geo-rectified. The attribute tables were exported out of ArcMap and into Excel where the sums of the different classes were determined. This allowed for a quantitative understanding of the vegetation recovery.

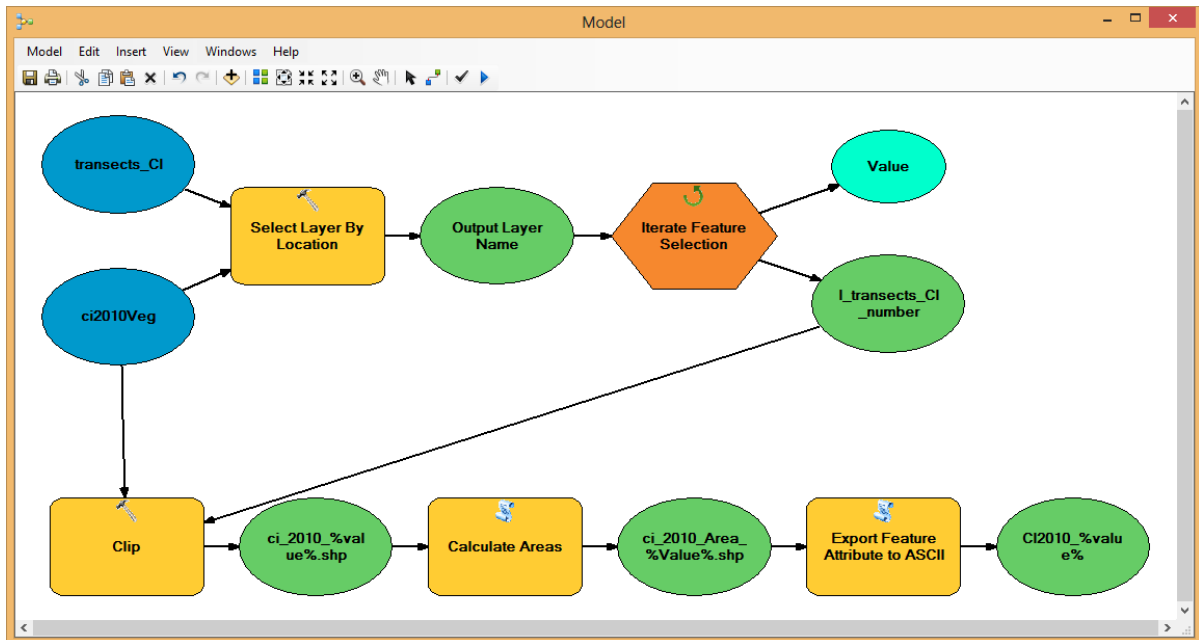


Figure 2.6 GIS Model. A screen shot of the GIS model used to extract the vegetation measurements from the transects in ArcMap.

## 2.5 Spatial Frequency

The spatial series that was obtained by the GIS model builder tool were analyzed to determine the frequency of repeated patterns along the island. Statistica was used to run spectral analysis on the spatial series. Spectral analysis uses the Fourier transformation to relate the spatial series to the frequency domain. The Fourier transformation breaks the spatial series into multiple sine waves. The component sine wave frequencies are represented as peaks in the frequency domain when plotted against the frequency spectrum. The peaks for each time series were counted by distance. The frequencies were compared each year to determine if they are consistent overtime and to determine if the alongshore variation in vegetation recovery is the same as the alongshore variation in storm impact that was described in Houser et al. (2008).

## 2.6 Biogeomorphic Recovery Model

The Verhulst (1838) population growth model was used to model the vegetation recovery. This model has been a foundation piece in the way that modern science understands population behavior. The model requires three inputs,  $r$  which is the growth rate of the vegetation,  $k$  which is the population limit of the vegetation, and  $N_0$  which is the amount of vegetation immediately following the disturbance. This study returned to the original population model. The number of plants cannot be counted because the study uses aerial imagery, so the area covered was used as a proxy for plant count. Both  $r$  and  $K$  were being tested for to find the combination that fit the observed vegetation recovery the most accurately. The  $K$  value was based on the available area for the vegetation to grow for each transect, when possible the pre Opal vegetation extent was used as the  $K$  value. This did not always provide the best fit with the observed vegetation recovery, in which case a higher  $K$  was chosen, lower  $K$ 's were not used as the area had been observed to support that much population it did not make sense to shrink the carrying capacity.

The post Opal and Post Ivan recovery times were overlapped in order to increase the number of recovery observations being compared to the model. A model of the averages for FP and SR was created as well as models of the individual transects. In order to determine if the model was a statistical significance predictor of the vegetation recovery a regression analysis was run on the differences between the predicted vegetation extents and the observed vegetation extents.

## 3 RESULTS

### 3.1 Study Area 1: Fort Pickens

#### 3.1.1 Average Recovery

When the average vegetation extent of FP is examined over time it is apparent that Hurricanes Opal and Ivan had the greatest impact on the vegetation (Figure 3.1.) In order to model the vegetation recovery, these two storms were used as the time 0 in the model. The years since disturbance were then plotted against the observed vegetation extents (Figure 3.2). When modeling the entire FP study area the Pre Opal vegetation extent worked well as the upper limit for the population ( $K$ ). When modeling individual transects the  $K$  that best fit the data were used. When all of the transects are examined as a whole the outliers are able to counterbalance each other, but when the individual transects are examined there is a greater chance of running into situations that do not follow the same trend.

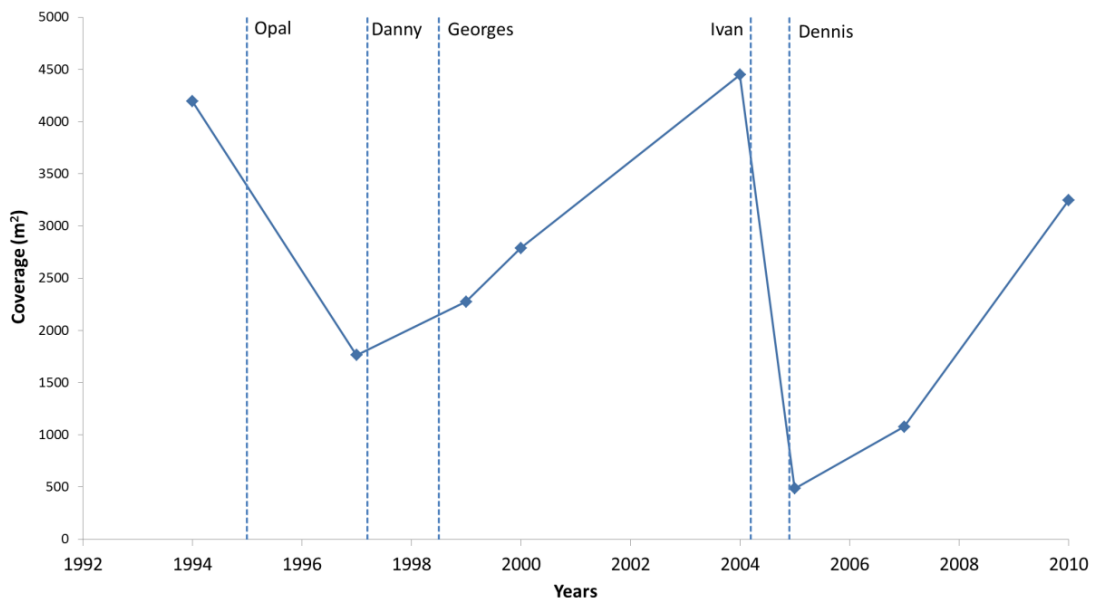


Figure 3.1 Fort Pickens Average Recovery. The averages of the vegetation measurements in the transects along the Fort Pickens study area are displayed along a timeline with the hurricanes that occurred during the study period being displayed in relation to the observations.

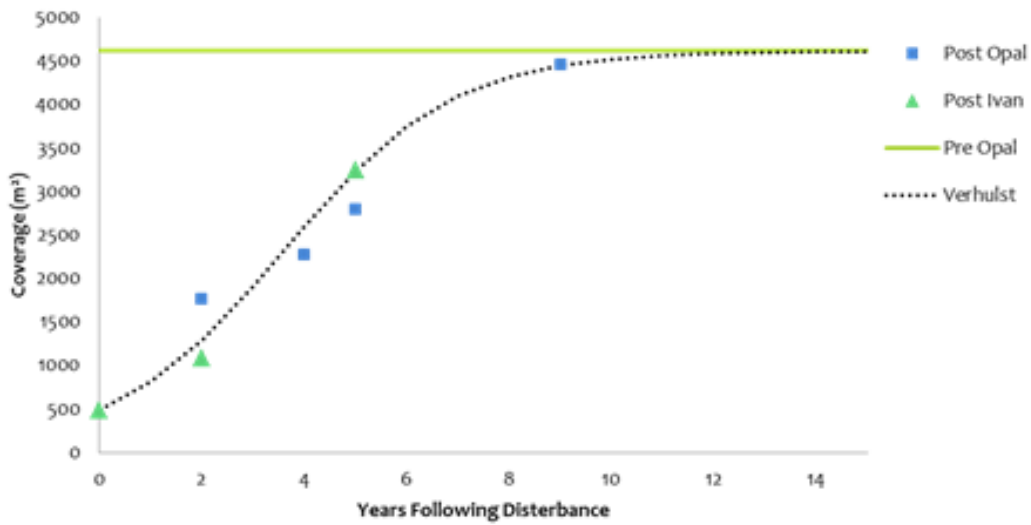


Figure 3.2 Verhulst Model of Fort Pickens. The Verhulst model was applied to the alongshore averages of the observed vegetation recovery. The model is statistically significant with a  $p < 0.01$ . The K value was the same as the Pre-Opal vegetation extent and the vegetation growth rate ( $r$ ) was 0.6. The vegetation recovery's maximum inflection point is at 6 years. The kick point was at 2 years.

### 3.1.2 Geomorphic Regimes

Examining the study area as a single feature overlooks the importance of geomorphic control regimes. Segments of FP fit well into the Sallenger (2000) model when the alongshore variation of vegetation recovery ( $r$ ) and  $K$  were modeled. Most notably in the overwash regime segments of the island Georges was destructive enough that it was used as the time 0 instead of Opal (Figure 3.3). This is the same area that the vegetation is spreading the most quickly. This corresponds with Stallins and Parker (2003) observation that the vegetation growing on washovers was better adapted to recolonizing disturbed areas than the vegetation on other landforms. The percent of the area in each transect that was used as  $K$  along the island does not have as clear of a relationship with the geomorphic control regime, although it appears that it is the transitional areas between the two regimes that can support the greatest amount of vegetation (Figure 3.4). The relationship between geomorphic control regime and the  $r$  and  $K$  values is most apparent when  $r$  and  $K$  are plotted with one another (Figure 3.5). The transects that have  $K$  and  $r$  values within 0.4 of each other are highlighted and appear to be collision regime.



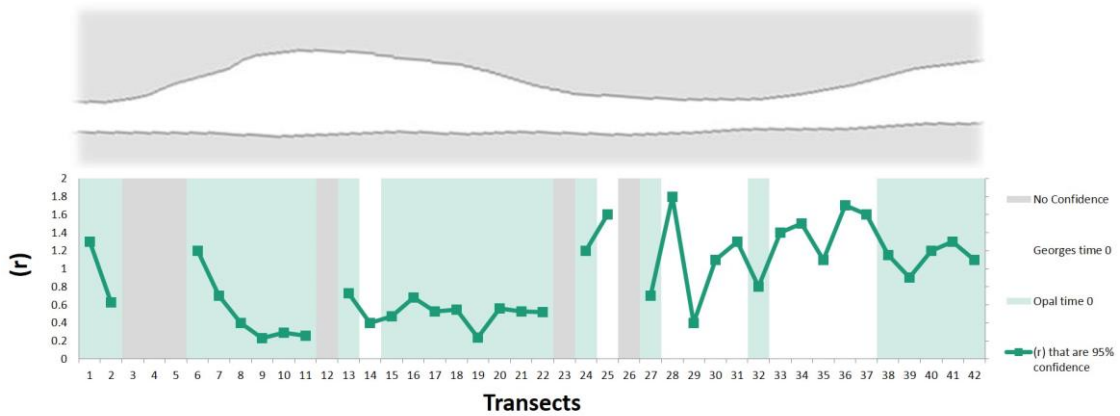


Figure 3.3 Alongshore Variation in  $r$  at Fort Pickens. The vegetation growth ( $r$ ) along the island (Blue line) varies with the geomorphic control regime. The narrow washover segment has high rates of vegetation growth and the wide collision regimes have low rates of vegetation growth. The light blue bars show the transects where Opal and Ivan were used as the two disturbance events, and the white transects show where Georges and Ivan were the two disturbance events.

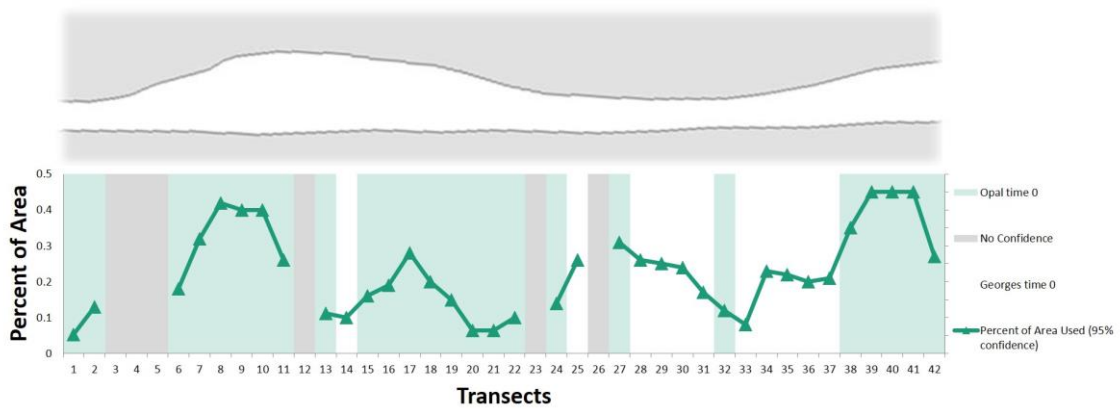


Figure 3.4 Alongshore Variation in  $K$  at Fort Pickens. The percent of the area in each transect that was used as  $K$  along the island (Blue line). The light blue bars show the transects where Opal and Ivan were used as the two disturbance events, and the white transects show where Georges and Ivan were the two disturbance events.

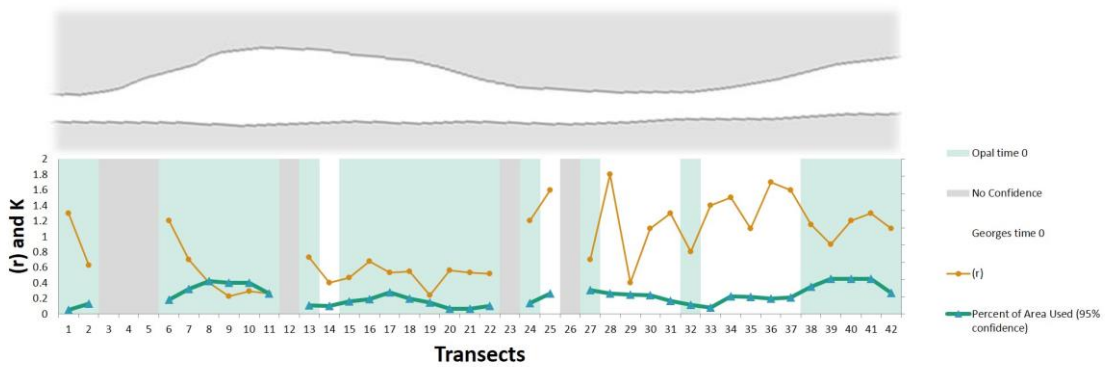


Figure 3.5 Alongshore Variation in  $r$  and  $K$  at Fort Pickens. The relationship between geomorphic control regime and the  $r$  and  $K$  values. The transects that have  $K$  and  $r$  values within 0.4 of each other are highlighted and are mostly in collision regime sections of the island.

Similarly when the recovery time of the study area is examined along the island the overwash and collision regimes are apparent (Figure 3.6). There is a gap between the predicted recovery times of the vegetation extent and the time at which the vegetation reaches the pre Opal vegetation extent in the collision regime.

The  $K$  in the overwash regime was more consistently the same as the pre Opal vegetation extent which means that the recovery times are the same. The recovery to pre Opal along the island shows that vegetation recovers in fewer than 5 years this corresponds with the collision regime locations where less vegetation was destroyed. The recovery time in overwash segments of the island where almost all of the vegetation was removed was between 5 and 10 years. The greatest recovery times are seen on the east side of the cusped head land where the two geomorphic regimes meet. This may be a result of the vegetation in this location being the same composition as the vegetation on the collision regime, but the dune system receiving more damage due to its proximity to the more vulnerable overwash segments.

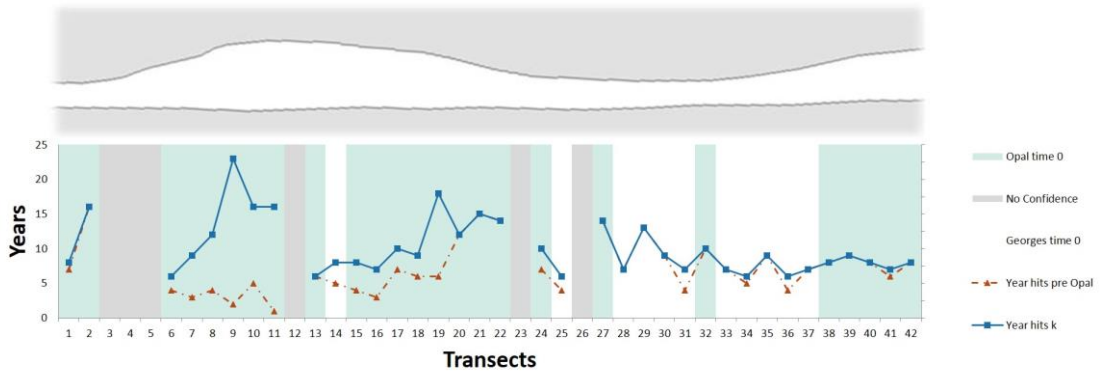


Figure 3.6 Alongshore Variation in Recovery Times at Fort Pickens. The figure shows the gap between the predicted recovery times of the vegetation extent (Blue line) and the time at which the vegetation reaches the pre Opal vegetation extent (Red line). The light blue bars show the transects where Opal and Ivan were used as the two disturbance events, and the white transects show where Georges and Ivan were the two disturbance events.

## 3.2 Study Area 2: Santa Rosa Island

### 3.2.1 Average Recovery

The vegetation coverage of SR during the study period indicates that Hurricane Ivan was responsible for more damage than hurricane Opal (Figure 3.7). Hurricanes Danny and Georges did not considerably decrease the vegetation extent but do appear to have prevented recovery. When the Verhulst model is applied to the vegetation coverage following hurricane Ivan and Georges as time 0 the fit is poor with an  $r^2$  of 0.36, but there is a large gap between the observed vegetation extents following Ivan's recovery and Georges' recovery (Figure 3.8). When the Verhulst model is applied to hurricanes Opal and Ivan as time 0 the fit is statistically significant with a  $p < 0.01$  and an  $r^2$  of 0.74 (Figure 3.9).

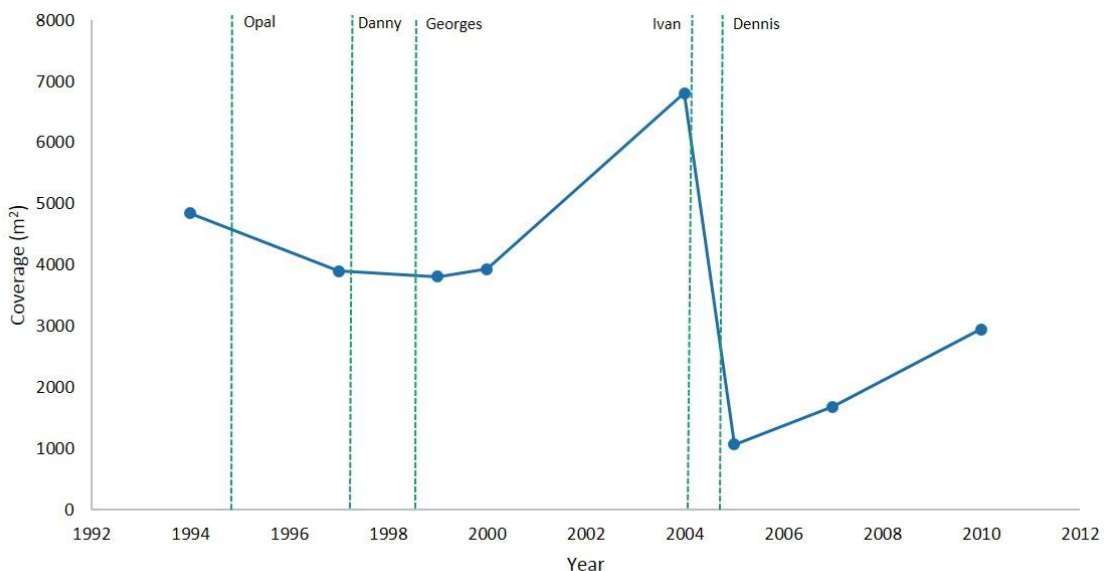


Figure 3.7 Santa Rosa Average Recovery. The averages of the vegetation measurements in the transects along the Santa Rosa study area are displayed along a timeline with the hurricanes that occurred during the study period being displayed in relation to the observations.

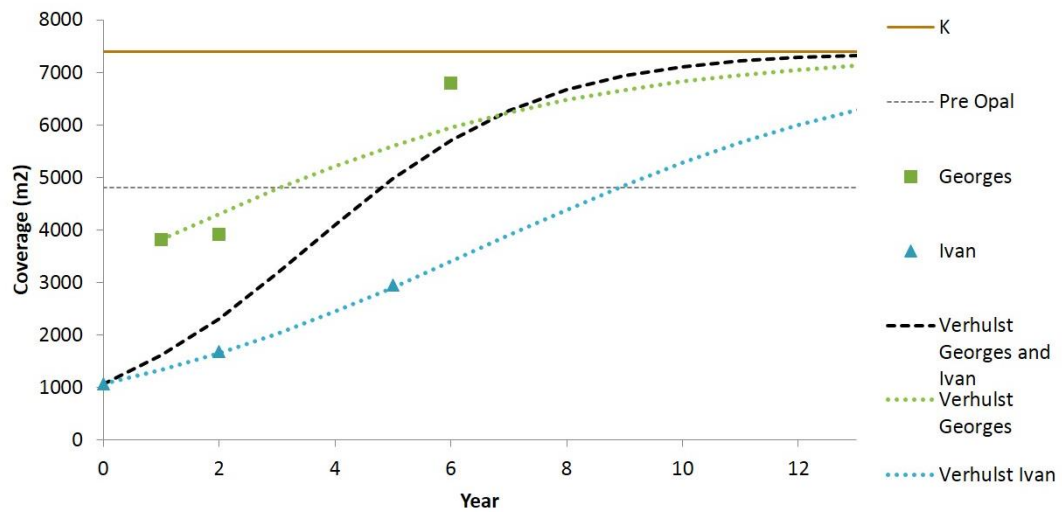


Figure 3.8 Hurricanes Georges and Ivan as Time 0 in Verhulst Model. The Verhulst model has poor fit with an  $r^2$  of 0.36. When the recovery following Georges and Ivan are broken out into two separate recoveries the Ivan recovery is significant with a  $p < 0.01$  and the Georges recovery is insignificant with a  $p < 0.13$ . The K value was 20% of the land in the transects and the vegetation growth rate ( $r$ ) was 0.27 following Ivan.

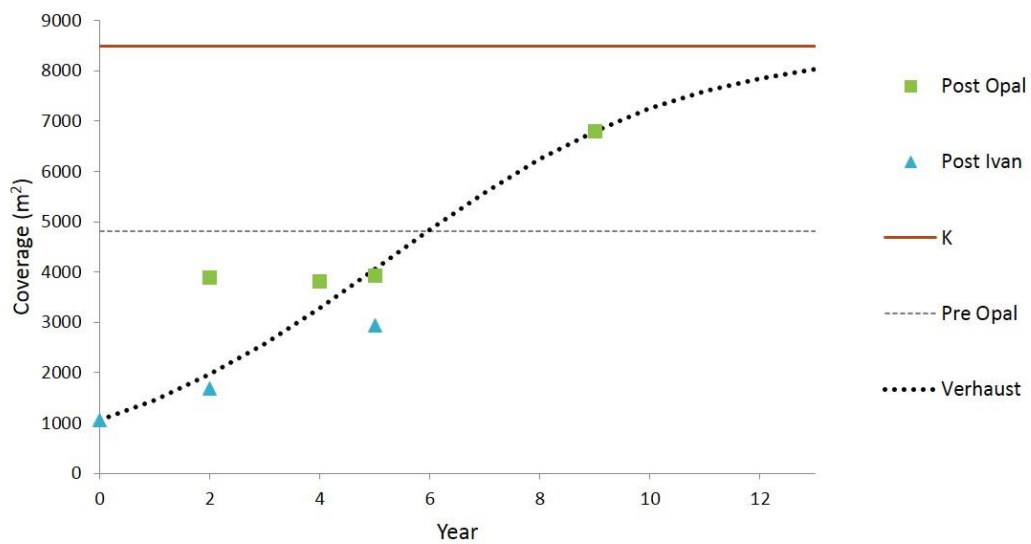


Figure 3.9 Hurricanes Opal and Ivan as Time 0 in Verhulst Model. The model is statistically significant with a  $p < 0.01$ . The K value was 23% of the land in the transects and the vegetation growth rate ( $r$ ) was 0.37.

The SR study area is made up of 154 transects. Of these transects 75 are significant fits and 79 are insignificant. There is a very strong relationship with the significance of the individual transects fit to the vegetation recovery model and which end of the study area is being examined. There are only two significant transects in the first 49 transects on the west end of the study area.

The west end is bordered by a more heavily populated area than the east end of the study area. The west end is owned and managed by the University of West Florida. This area of the island also supports more marsh and maritime forest communities. Many of the transects with the poor fit were a part of the marsh reconstruction project and shrimp farming ponds that were slowly filling in during the study period. Without field verification of the vegetation types during the study it is difficult to say with certainty why there is such a significant difference between the western half of SR and the eastern half, but the dominant vegetation types on the western end appear to be shifting away from low, burial intolerant species associated with marsh to the burial tolerant stabilizers and dune builders associated with dunes. The change in the plant types that dominate the area would then change the  $r$  of the vegetation recovery.

When transects 0 to 42 are excluded from the average vegetation coverage per  $m^2$ , the impact of Opal and Georges increases (Figure 3.10). The fit of the model has a  $p$  value  $< 0.01$  that is significant (Figure 3.11). The best fit  $K$  is more than double the height of the height of the pre Opal vegetation. The pre Opal  $K$  is  $3000 m^2$  less than the pre Ivan vegetation coverage (Figure 3.12). The pre Ivan vegetation could be used as the  $K$ , but the Verhulst model does not fit the measured vegetation extent well at the pre

Ivan measurement (Figure 3.13). This may indicate a change in the dominant geomorphic control, such as fewer washovers, but more likely it is the result of the shrinking area of the marsh and forest in the entire study area and an increase in back island dunes. This is an area where additional comparisons to dune profiles during the same time would be informative. The difficulty in defining K comes from the same dilemma as defining recovery, it is based on the concept that there is a state of equilibrium, but if the area being studies is not currently in an equilibrium state it is difficult to say with certainty where that point would be.

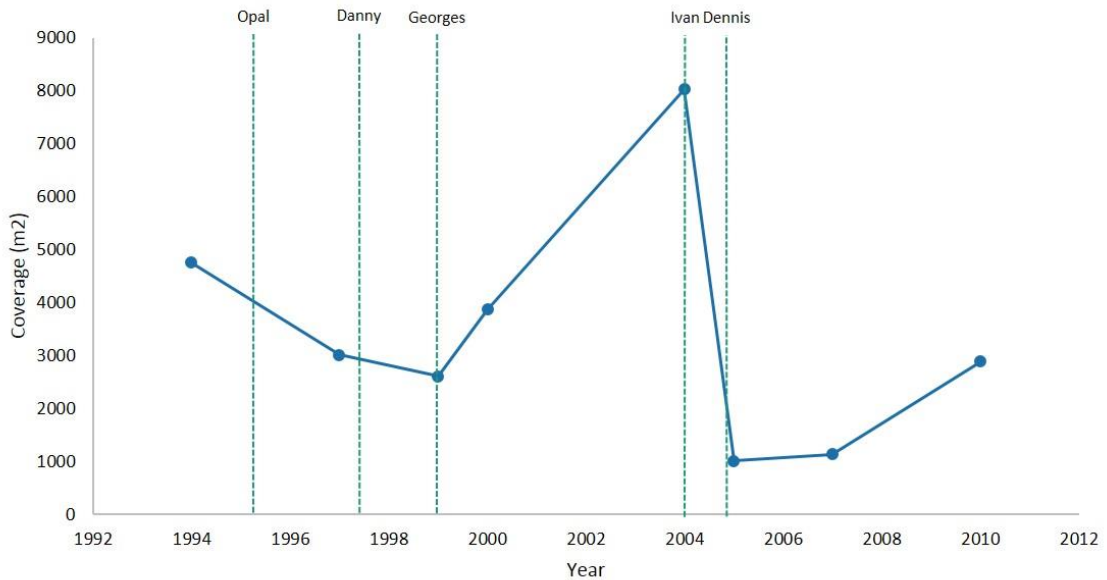


Figure 3.10 Santa Rosa Transects 43 - 153 Averages Vegetation. The averages of the vegetation measurements in the transects from 43 to 153 in the Santa Rosa study area are displayed along a timeline with the hurricanes that occurred during the study period being displayed in relation to the observations.

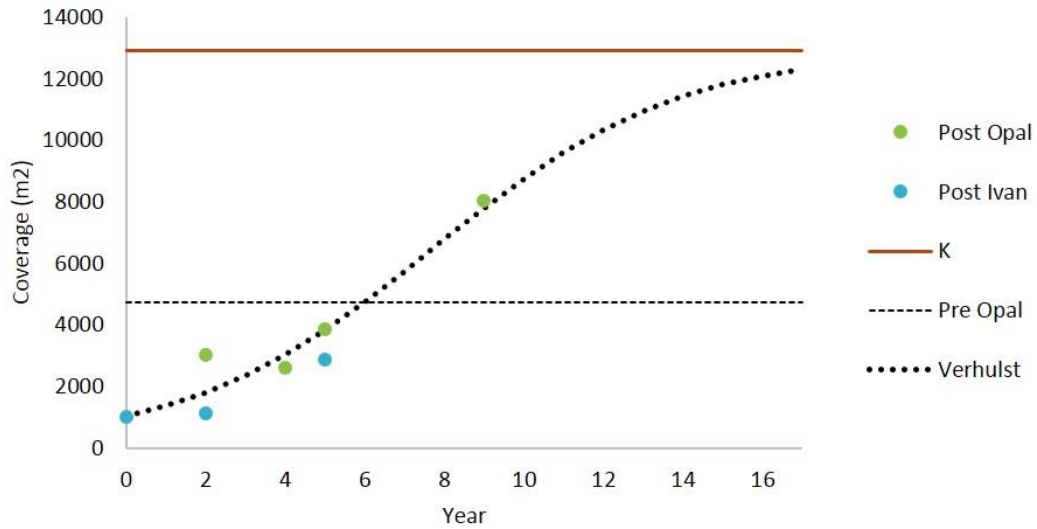


Figure 3.11 Santa Rosa Verhulst Model Best Fit K. Hurricanes Opal and Ivan were used as the time 0 in the Verhulst model. The vegetation measurements are the averages of the transects from 43 to 153 in the Santa Rosa study area. The model is statistically significant with a  $p < 0.01$ . The K value was 33% of the land in the transects and the vegetation growth rate ( $r$ ) was 0.32. The vegetation recovery's maximum inflection point is at 11 years. The kick point was at 5 years.

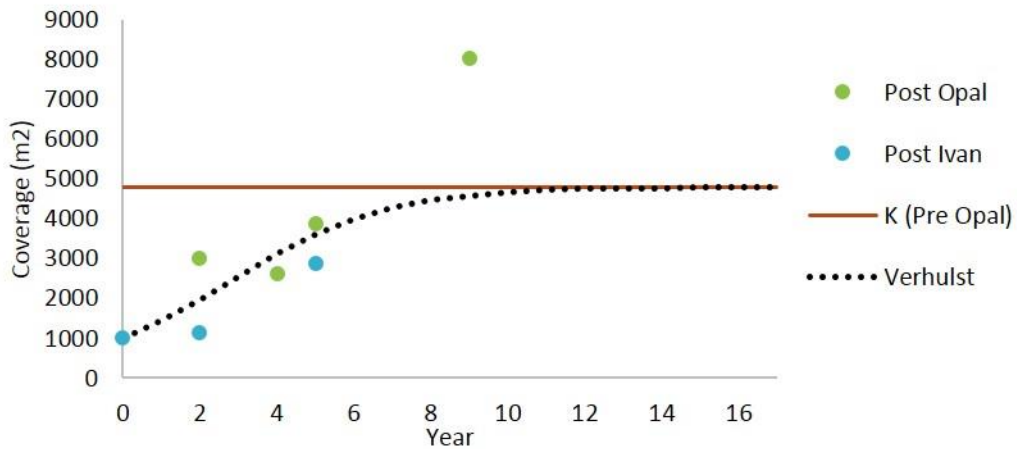


Figure 3.12 Santa Rosa Verhulst Model Pre Opal K. Hurricanes Opal and Ivan were used as the time 0 in the Verhulst model. The vegetation measurements are the averages of the transects from 43 to 153 in the Santa Rosa study area. The model is statistically significant with a  $p < 0.02$ . The K value was the pre Opal Vegetation coverage and the vegetation growth rate ( $r$ ) was 0.49. The vegetation recovery's maximum inflection point is at 5 years. The kick point was at 2 years.



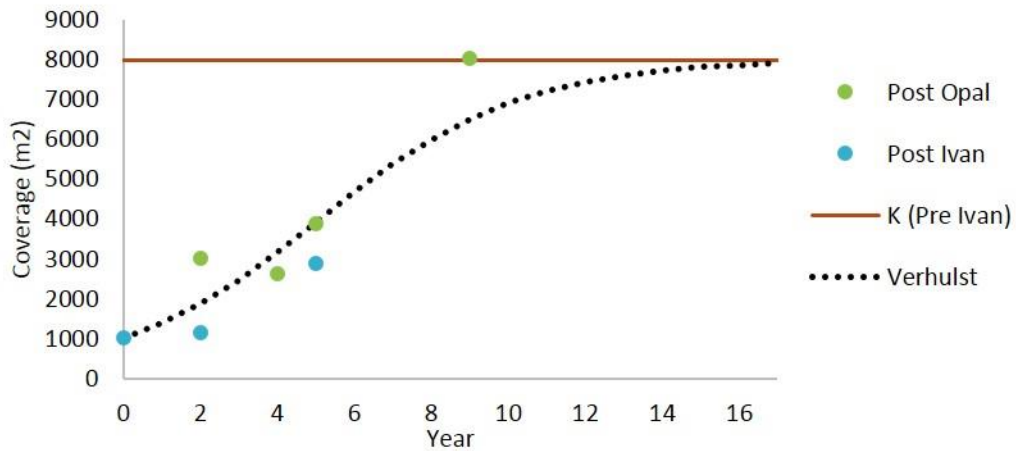


Figure 3.13 Santa Rosa Verhulst Model Pre Ivan K. Hurricanes Opal and Ivan were used as the time 0 in the Verhulst model. The vegetation measurements are the averages of the transects from 43 to 153 in the Santa Rosa study area. The model is statistically significant with a  $p < 0.01$ . The K value was the pre Ivan vegetation coverage and the vegetation growth rate ( $r$ ) was 0.38. The vegetation recovery's maximum inflection point is at 8 years. The kick point was at 3 years.

### 3.2.2 Geomorphic Regimes

The strong relationship between the difference in predicted time to recovery and observed time to recovery to the geomorphic control regime is considerably less evident in the SR segment, although transects 49-59 exhibit the a large divide between  $r$  and  $K$ , but it is less distinct than the divide in the overwash dominated transects in FP (Figure 3.14). This can in part be explained by the fact that the pre Opal vegetation and  $K$  were not the same in SR the way they were in FP. The recovery to  $K$  and to pre Opal vegetation in the overwash regime transects are not as close in SR as they are FP. The collision regime transects make up a greater proportion of SR than on FP, they have characteristically wider divides between the recovery to  $K$  and to pre Opal vegetation as seen in transects 134-137 (Figure 3.15).

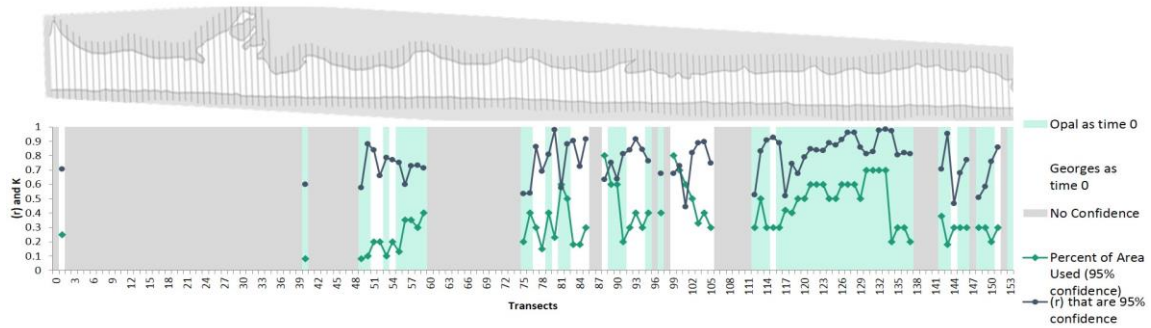


Figure 3.14 Alongshore Variation in  $r$  and  $K$  at Santa Rosa. The relationship between geomorphic control regime and the  $r$  and  $K$  values. The transects that have  $K$  and  $r$  values within 0.4 of each other are highlighted and are mostly in collision regime sections of the island.

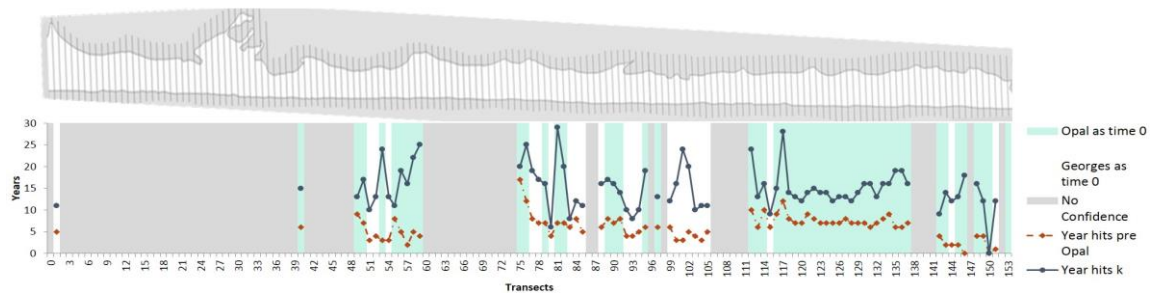


Figure 3.15 Alongshore Variation in Recovery Times at Santa Rosa. The figure shows the gap between the predicted recovery times of the vegetation extent (Red line) and the time at which the vegetation reaches the pre Opal vegetation extent (Green line). The light blue bars show the transects where Opal and Ivan were used as the two disturbance events, and the white transects show where Georges and Ivan were the two disturbance events. The transects that did not have significant fits to the population model are grey and had either drastically different recovery rates following the two storms or the population had a large drop between the 2 and 3 measurements.

The majority of the transects that did not have significant fits were dominated by marshy vegetation. The transects that exhibited significant fits were in areas with more dunes. The growth rates are relatively consistent in all of the significant transects (Figure 3.16). The portions of SR that were more impacted by Georges than Ivan tend to use a smaller percent of the available area than the transects that were more resistant to the second storm (Figure 3.17).

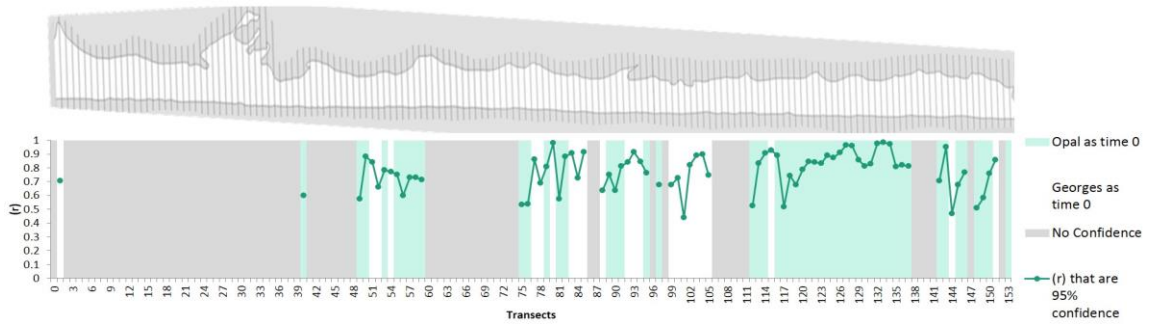


Figure 3.16 Alongshore Variation in  $r$  at Santa Rosa. The vegetation growth ( $r$ ) along the island (green line) varies, the few wash over segments have more sporadic growth rates than the collision regimes. The light green bars show the transects where Opal and Ivan were used as the two disturbance events, and the white transects show where Georges and Ivan were the two disturbance event. The transects where the confidence level was under 95% are grey.

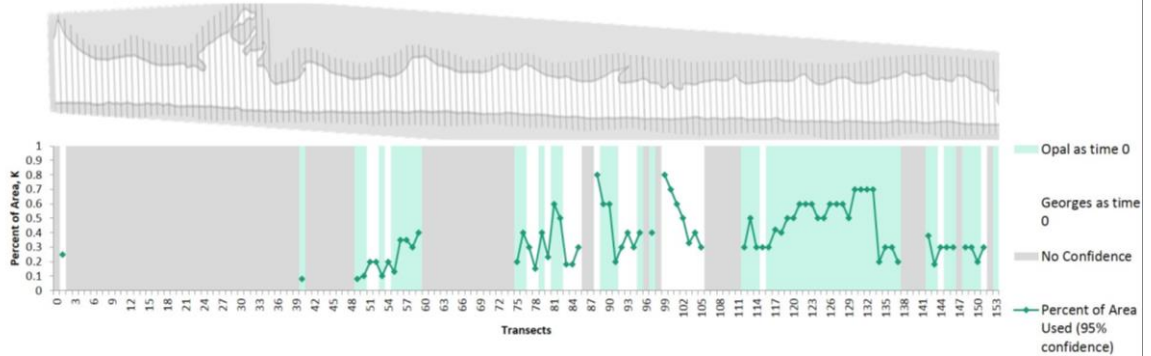


Figure 3.17 Alongshore Variation in  $K$  at Santa Rosa. The percent of the area in each transect that was used as  $K$  along the island (green line). The light green bars show the transects where Opal and Ivan were used as the two disturbance events, and the white transects show where Georges and Ivan were the two disturbance events. The transects where the confidence level was under 95% are grey.

### 3.2.3 Spatial Frequencies

The results of the Fourier transformation of the eight vegetation density spatial series were compared to determine what distance the greatest number of peaks were occurring. Peaks were counted if they were a greater density than the frequencies immediately before or after and not based on the relative magnitude of the peak. The distances that had the greatest number of peaks were at 7,700, 1,400, 670, and 342 meters (Figure 3.18). When only the post storm data was examined the peak overlaps occurred at the same frequencies that the majority of spatial series experienced, although the densities in the 2005 data are weaker than those in the 1997 data that it is difficult to tell how meaningful any peaking in the 2005 data is to connecting the damage to the ridge and swale bathymetry (Figure 3.19). The pre storm data only overlapped with the common frequencies at 1400 meters, unlike the other series the pre-storm years peaked at 3850, 616, and 256 meters (Figure 3.20). 1400 m is significant because this is the length scale where cusped forelands and transverse ridges exhibit an alongshore variation (Houser et al. 2008).

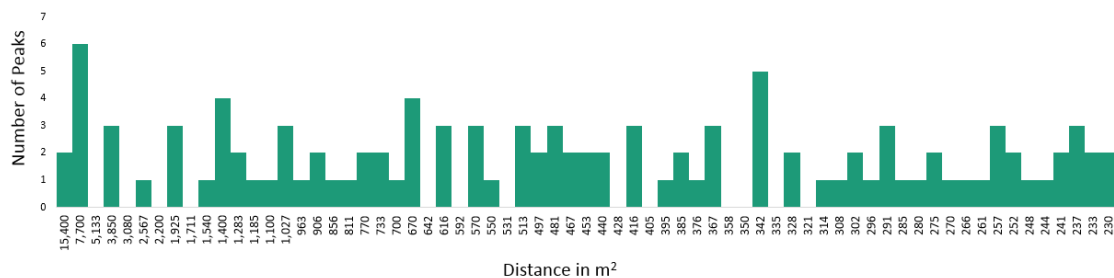


Figure 3.18 Fourier Transformation Peak Counts. All eight spatial series of SR’s peaks were counted and plotted against distances to identify clumping of peaks.

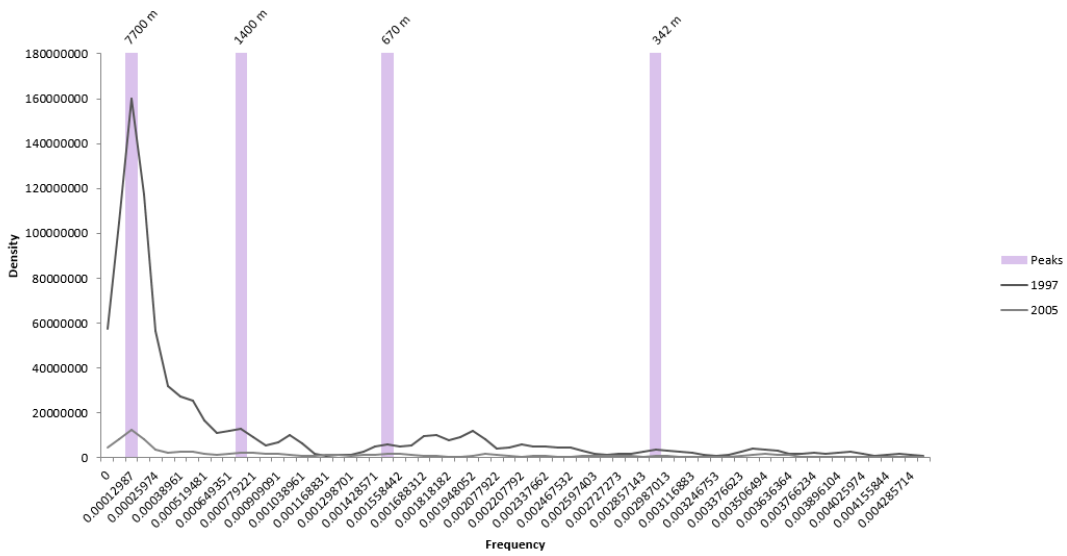


Figure 3.19 Fourier Transformation Post Storm. The frequencies of the post storm spatial series of SR are compared. The purple indicates where both series are peaking.

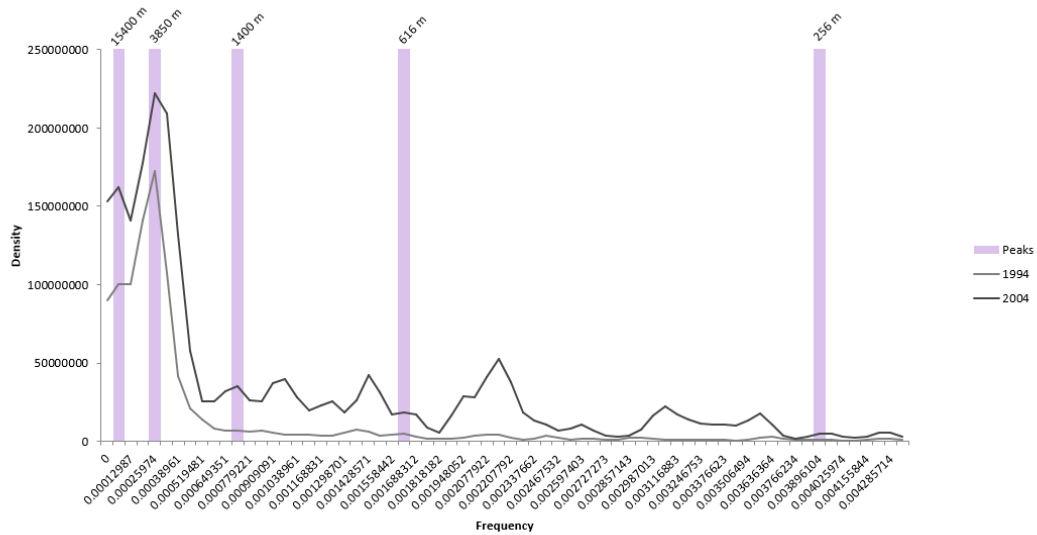


Figure 3.20 Fourier Transformation Pre Storm. The frequencies of the pre storm spatial series of SR are compared. The purple indicates where both series are peaking.

## 4 DISCUSSION

The study is the first to characterize the rates of vegetation recovery on a barrier island following a hurricane or tropical storm using the Verhulst model. Specifically this study determines the spatial frequency at which greater vegetation damage occurs and its relation to the geomorphic controls to physical characteristics of the barrier island (Houser et al., 2008, Sallenger, 2000). The biogeomorphic vegetation recovery model that describes the recovery at data points along the island was evaluated for the spatial variations in the vegetation growths dependence on the dominate geomorphic control regime. Increased understanding of the response of islands after storms will allow policy makers to make more informed decisions when deciding how and where to focus storm recovery efforts. Escambia County, Florida, was advised to spend nearly half a million dollars on re-vegetation efforts alone following relatively minor damage during the 1998 hurricane cycle (Leadon, 1999).

### 4.1 Implications of Changing Storm Frequencies

Stone et al. (2004) noted that the beach in the FP study area did not begin to recover from Hurricane Opal until 6 years following the storm. When compared to the modeled vegetation recovery, year 6 is when the recovery is moving out of an exponential increase and is beginning to level out as it approaches K. The implication is that the near recovery of the vegetation in the study area has allowed for the beach and

dunes to begin recovery (Figure 3.2). The modeled results indicates that the vegetation on the overwash regime dominated FP is resilient to storm intervals greater than or equal to ten years (Figure 4.1). The major overwash inducing storms that occurred during the study period were around a ten year interval, with Opal in 1995 and Ivan in 2004.

Unlike FP where the overwash regime transects vegetation is predicted to recover before the next 10 year storm cycle. The washover segments of SR have a larger gap between reaching pre Opal vegetation extent and reaching K than the collision regime segments of SR (Figure 3.11). The model indicates that the vegetation on the collision regime dominated SR is resilient to storm intervals greater than fifteen years (Figure 4.2). The greatest difference between FP and SR is seen at 5 years, in FP the vegetation growth is at its greatest and is about to begin slowing, but in SR the vegetation growth is only beginning to hit its maximum rate. The vegetation recovery of SR when compared to FP reinforces Houser and Hamilton's (2009) suggestion that FP is better adapted to higher frequencies of storms than SR. This is most evident in the greater damage following Ivan despite greater vegetation coverage prior to the storm, this suggests that the vegetation communities were different before Opal and Ivan. The vegetation in overwash regime dominated areas is better adapted to a quick recovery than the vegetation in collision dominated transects. In this way the overwash regime dominated segments of the island are more resilient to the impacts of storms.

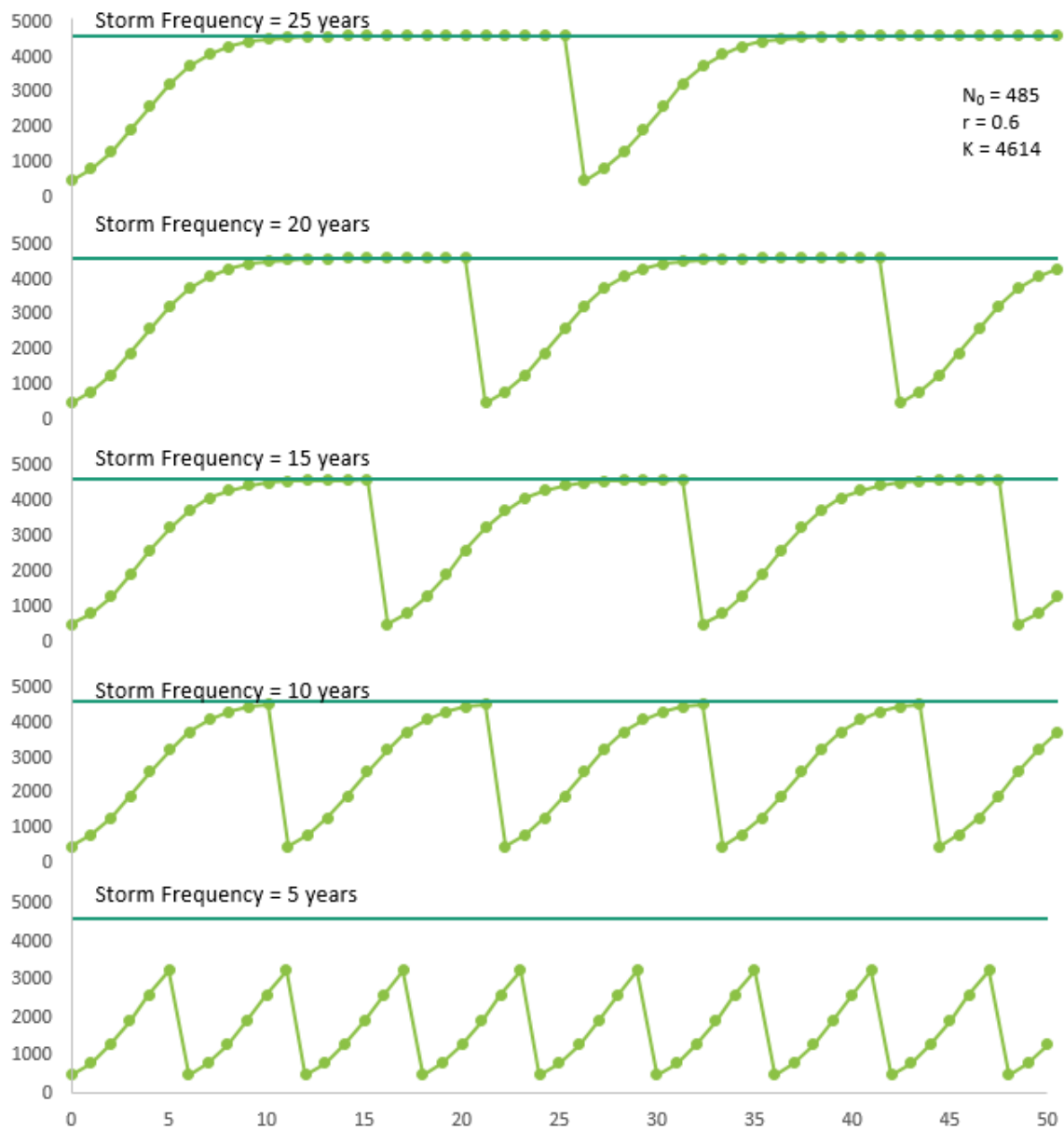


Figure 4.1 Recovery Time Series Based on Fort Pickens  $r$  and  $K$ . The figure examines the recovery at different storm frequencies assuming that the  $K$  and  $r$  that were found from the Opal and Ivan recoveries of FP did not change.



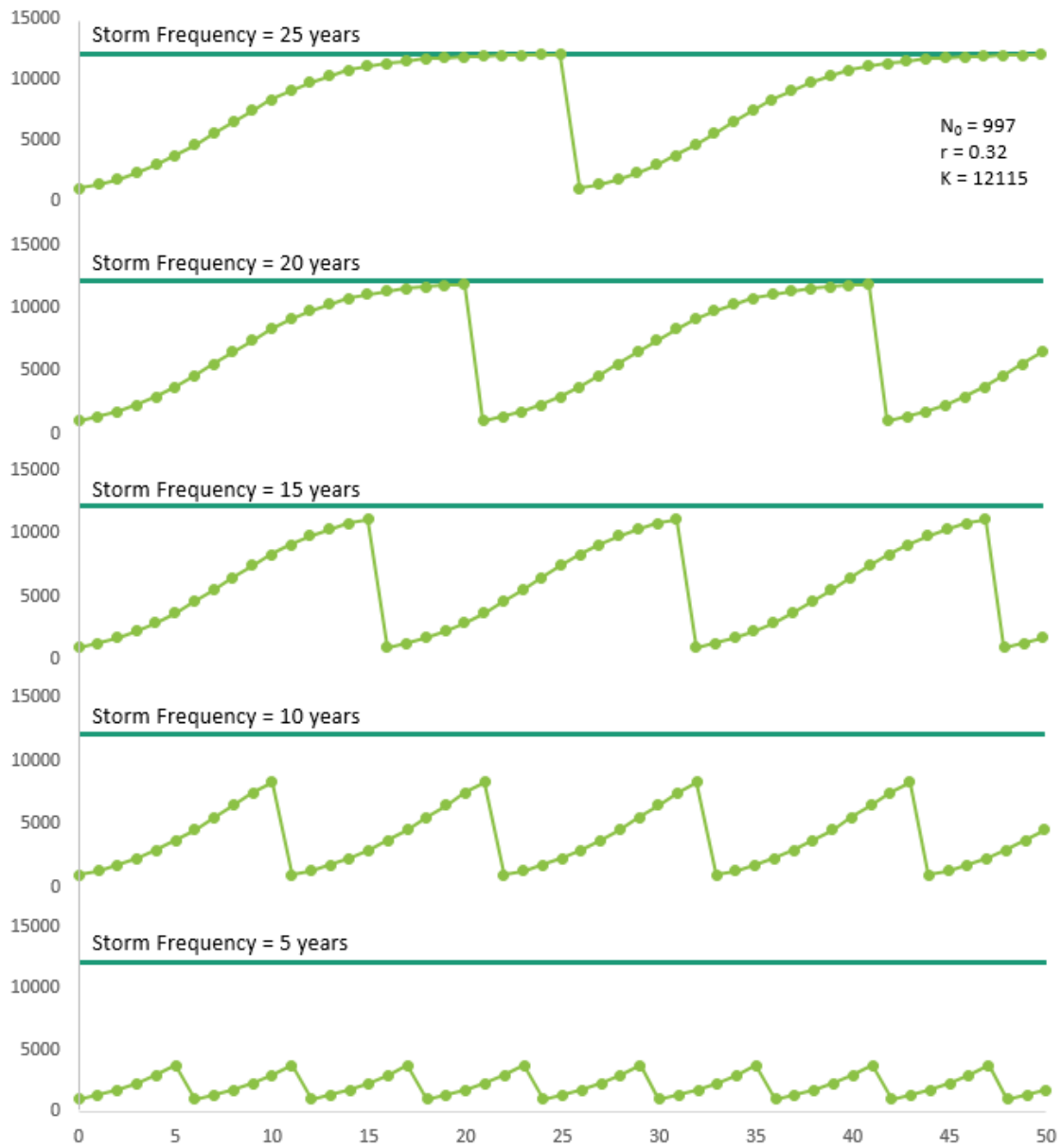


Figure 4.2 Recovery Time Series Based on Santa Rosa  $r$  and  $K$ . The figure explores the recovery at different storm frequencies assuming that the  $K$  and  $r$  that were found from the Opal and Ivan recoveries of SR did not change.

## 4.2 Implications of Changing Storm Magnitudes

The problem with these calculations of the islands recovery time is that they assume that the impact of storm always causes overwash and that the storm impact is the same for all storms. In reality though, the size of storms fluctuate, causing variations in the setup of the storm. During the study period there were more than the two major storms that were used as time 0, Hurricane Georges was a large storm that was used in some of the transects. The wave setup for Georges was smaller than the wave setup for Ivan at 1m versus the 1.2m (Stone et al., 2004, Claudino-Sales et al., 2010). Hurricane Georges did cause damage, but it was most noticeable in the areas that are more prone to overwash due to smaller dunes or a shallow beach face (Figure 3.3).

The variations in storm size impact the distance that overwash is able to travel inland or if it occurs at all. On SR 8% of the K level of vegetation survived Hurricane Ivan, if a storm of the same strength were to hit the island every ten years the vegetation would never reach the K level, but if there was a ten year frequency where 92% of the K vegetation level remained the vegetation would reach the K level well before the next storm (Figure 4.3). The problem then becomes one of conflating the storm frequency with the storm intensities. When a storm occurs while the vegetation is still recovering from a previous storm it is as if the storm that hits is a magnitude greater than it would be if the island had recovered (Figure 4.5).

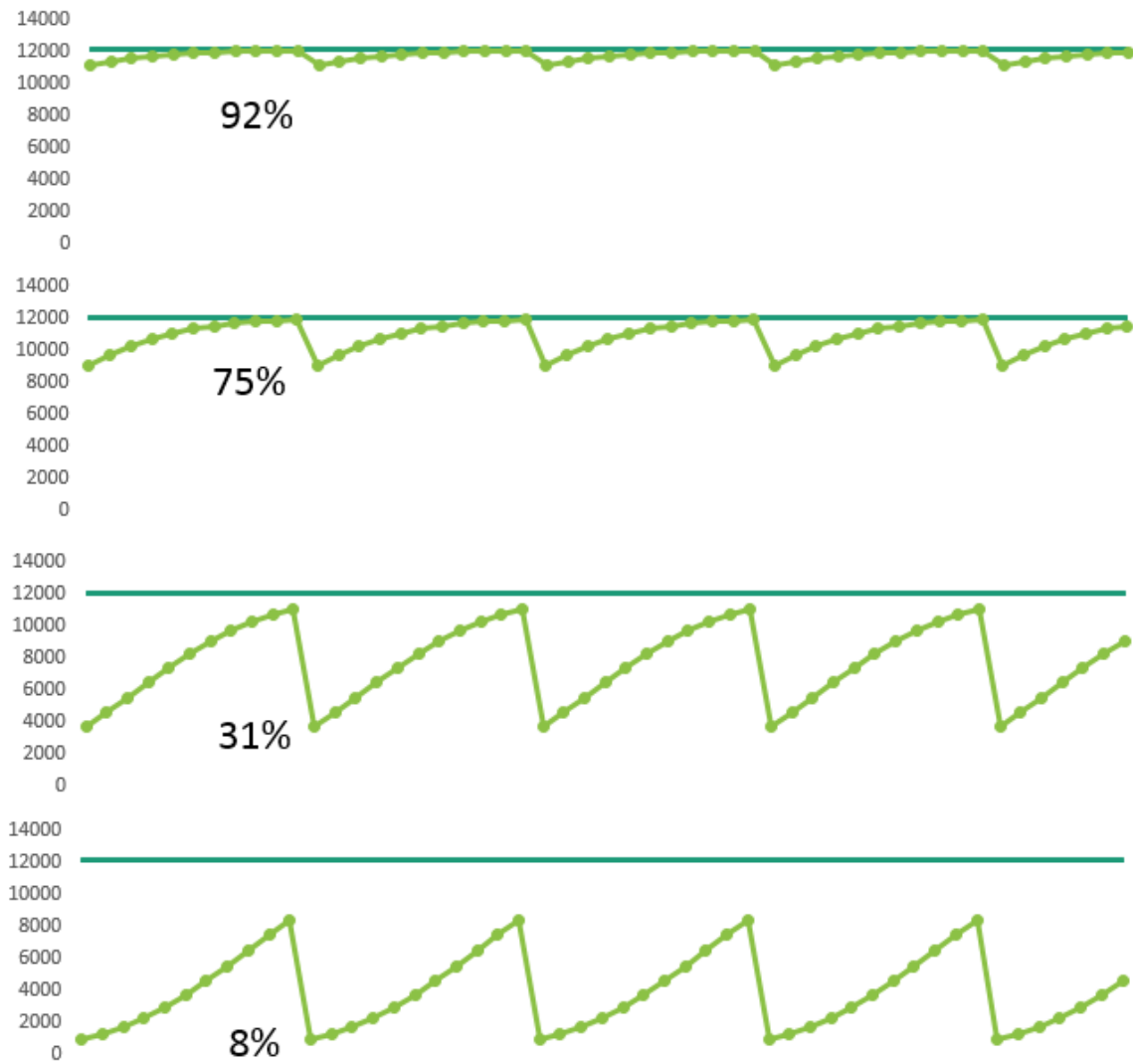


Figure 4.3 Recovery to Different Storm Intensities. The figure examines the recovery at different storm intensity assuming that the K and r that were found from the Opal and Ivan recoveries of SR did not change.

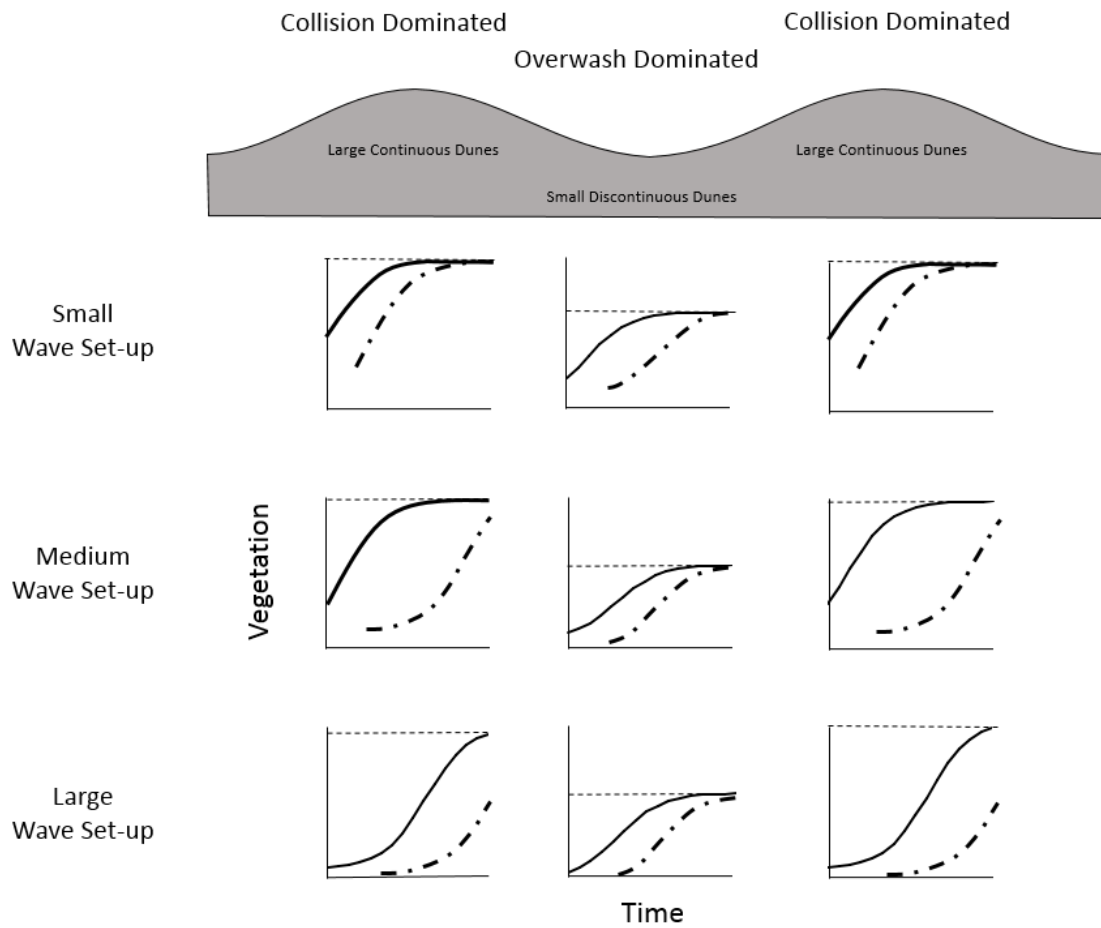


Figure 4.4 Conceptual Model of Recovery Drivers. When simplistically envisioned the recovery rate of vegetation following minor storms will be fastest in the headlands that's are geomorphically dominated by a collision regime and slightly slower in the washover fans. Following medium storms the amount of time needed for recovery between the geomorphic regimes will be similar because the growth rate of the vegetation on the overwashed areas is higher and the vegetation on the collision regime portions of the island have greater vegetation survival. Following large storms recovery will be fastest in the overwashed areas because the vegetation spreads quickly and the area has a lower carrying capacity, where the vegetation in the headlands has a lower growth rate and has a larger area to repopulate. The dotted line represents what the vegetation recovery becomes when a second storm hits before the vegetation has a chance to recover to K.

### 4.3 Similarities and Differences of FP and SR

The gap between the predicted recovery and observed recovery in collision regime portions of FP is in part the result of the loss of maritime forest and the infilling of the lakes that has increased the amount of suitable habitat for vegetation in these transects from 1995 to 2010 (Figure 3.6). This gap also appeared in the majority of the SR study area and was so strong on the western half of the study area that the vegetation model did not have any significant fits (Figure 3.15). Although both of these areas are experiencing changes in their dominant land covers, the use of the pre storm vegetation extent as a base line should also be questioned because of its poor performance on SR. The gap between the K and the pre storm vegetation extent suggests the vulnerability of the collision regime portions of the island, the vegetation that is behind the dunes is often very sensitive to disturbances.

Much of SR that was marsh in 1994 was overwashed and infilled during the storms that occurred during the study period. Although some marsh returned to these transects the majority are still less vegetated, but this has increased the area available for the dune building species as seen around SR transect 50 and 60 (Figure 4.5). The 2010 image shows a similar amount of dune vegetation present, but the vegetation is on the back part of the island and not near the beach like it was in 1994. Very little recovery of the foredune vegetation is observed in the collision or overwash regime transects. Houser and Hamilton (2009) attribute the vegetation's growth farther from the beach to the movement of seed banks and rhizomes by the overwash into the washover terraces.

The low recovery of the foredune vegetation in this location may also in part be explained by the removal of the road debris and the building of a new road.

Unlike SR the vegetation recovery in the overwashed transects in FP have high  $r$  values which are typical of low growing maintainer species (Figure 3.3). The more often that disturbances occur the fewer  $K$  adapted species will be present in the community. The washover area consistently experienced overwash events during the study time - which is why Georges was used as the time zero for these transects instead of Opal. The overwash area was commonly flooded similar to what Wolner et al. (2013) observed on Metompkin Island. This suggests that FP is similarly influenced by both physical and ecological processes. The plant species themselves reinforce the geomorphology that increases the likelihood of overwash.

On SR the low vegetation growth on the foredunes coupled with the  $K$  values that were greater than the pre storm vegetation indicates that the SR study area is not recovering between storm events. The model predicts vegetation recovery to occur 16 to 20 years following the event (Figure 4.2). This is twice as long as the recovery time observed in FP. This suggests two things: that SR is more susceptible than FP to the changing frequencies of storm events, and that SR will be undergoing a shift in species dominance that will more closely resemble that seen on the FP end of the island. As the plant species change to ( $r$ ) adapted species the dunes on SR will become less continuous, this in turn will increase the likelihood of overwash. A greater proportion of vegetation was removed from SR following Ivan than was removed following Opal (Figure 3.7). The difference in the vegetation suggests that SR is transitioning between the  $K$  adapted

builder species to the r adapted maintainer species that allow washover events to occur with smaller wave setup.

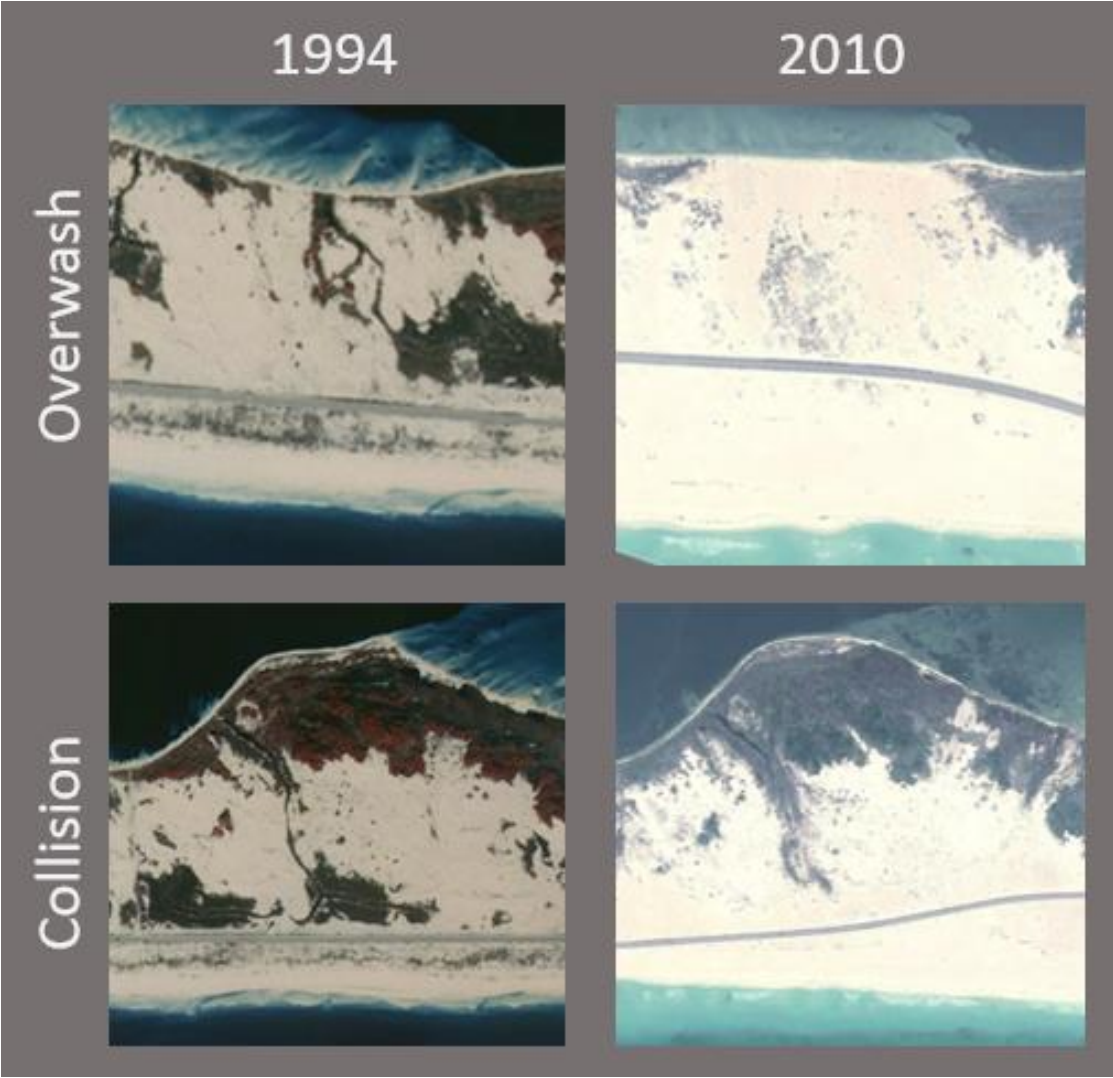


Figure 4.5 Vegetation Change between 1994 and 2010. The change between 1994 and 2010 of a washover area around transect 50 is shown at the top and of an erosional area is shown at the bottom around transect 60

#### 4.4 Implication for Future Works

Models of dune recovery such as Duran and Moore (2013) are overly focused on the geomorphic controls on the growth of the vegetation and do not take the vegetation's ability to alter their environment to meet their needs into account. The approach in this study is still a geocentric approach to vegetation and then dune recovery but is acknowledging the variability in the vegetation that is present in the environment. Future studies of dune vegetation recovery should be augmented with vegetation censuses to better understand the plant communities present. Other studies using aerial imagery should focus on the foredunes alone. The increasing availability of government collected LiDAR data sets also offers opportunities for integration of dune height and vegetation damage into the same study.



## 5 CONCLUSIONS

The results of this thesis have demonstrated that the Verhulst model may be used to describe vegetation recovery on a barrier islands. Until now vegetation recovery has often been a process that is overlooked in barrier island recovery studies. The measurement of vegetation recovery using aerial imagery has opened future studies to use fewer data points. Once the  $r$  or  $K$  have been determined for an area the recovery time could be determined by the amount of vegetation that survives the storm. In order to do this the  $r$  and  $K$  for a large variety of plant communities and geomorphic controls will need to be determined.

Use of remote sensing in conjunction with the Verhulst model exposes that on Santa Rosa Island vegetation growth rates ( $r$ ) are higher in the overwashed transects. The transects where there were vegetation was able to spread to a greater portion of the transect ( $K$ ) were collision dominated transects. The Verhulst model in these transect had lower vegetation growth rates ( $r$ ). It is the wider collision dominated transects that are more vulnerable to increased intensity of storms because their dunes are more dependent on the vegetation recovering than the vegetation growing on washover. The use of the Fourier transformation to relate the spatial series to the frequency domain reveals that there is an alongshore variation in the vegetation coverage before and after Opal and Ivan that corresponds to the frequencies of the ridge and swale bathymetry, around 1400 m.

At the current frequency and intensity of storms the west end of Santa Rosa, FP, is sufficiently adapted to recover its vegetation before the next overwash inducing storm. The western section, SR, is experiencing disturbances before it recovers from the earlier storm. This indicates that the wider, more collision regime controlled section of the island are more vulnerable to an increase in storm intensity than storm frequency. The vegetation in these sections may with time alter their species profiles to be more r adapted if the intensity and the frequency are both increasing, which will encourage the proliferation of low lying species that stabilize sand but do little to develop dunes. This in turn will encourage overwash to continue occurring. The slower recovery time of the dunes and vegetation allows the island to better react as a coherent unit to an increase in sea level at the same time that storm frequencies are increasing, this will help maintain the barrier island by moving the cusate sediment inland.

Attempts to prevent overwash could lead to the inundation of portions of the island as sea levels rise if the island is not allowed to adapt to changing conditions. When revegetation efforts are undertaken they should focus on increasing the sand stabilizers instead of dune builder to prevent the sediment from leaving the island.

## REFERENCES

- Amsberry, L. (2000). Clonal Integration and the Expansion of *Phragmites Australis*. *Ecological Applications*, 10, 1110-1118.
- Ayyad, M. A. (1973). Vegetation and Environment of the Western Mediterranean Coastal Land of Egypt: I. The Habitat of Sand Dunes. *Journal of Ecology*, 61, 509-523.
- Baas, A. & J. Nield (2007). Modelling Vegetated Dune Landscapes. *Geophysical Research Letters*, 34.
- Boyce, S. (1954). The Salt Spray Community. *Ecological Monographs*, 24, 29-67.
- Brodhead, John MB, & Godfrey, Paul J. (1979). *The Effects of Off-road Vehicles on Coastal Dune Vegetation in the Province Lands, Cape Cod National Seashore, Massachusetts*: Environmental Institute.
- Claudino-Sales, V., P. Wang & M. H. Horwitz (2008). Factors Controlling the Survival of Coastal Dunes during Multiple Hurricane Impacts in 2004 and 2005: Santa Rosa Barrier Island, Florida. *Geomorphology*, 95, 295-315.
- Claudino-Sales, V., P. Wang & M. H. Horwitz (2010). Effect of Hurricane Ivan on Coastal Dunes of Santa Rosa Barrier Island, Florida: Characterized on the Basis of Pre-and Poststorm LIDAR Surveys. *Journal of Coastal Research*, 470-484.
- Cleve, C., M. Kelly, F. R. Kearns & M. Moritz (2008). Classification of the Wildland–Urban Interface: A Comparison of Pixel-and Object-Based Classifications Using High-Resolution Aerial Photography. *Computers, Environment and Urban Systems*, 32, 317-326.
- Davidson-Arnott, R. (2010). *Introduction to Coastal Processes and Geomorphology*: Cambridge University Press.
- Disraeli, D. J. (1984). The Effect of Sand Deposits on the Growth and Morphology of *Ammophila Breviligulata*. *Journal of Ecology*, 72, 145-154.
- Duran, O, & Moore, L J. (2013). Vegetation Controls on the Maximum Size of Coastal Dunes. *Proceedings of the National Academy of Sciences*, 110(43). 17217-17222.
- Feagin, R, & Wu, X. (2007). The Spatial Patterns of Functional Groups and Successional Direction in a Coastal Dune Community. *Rangeland Ecology & Management*, 60(4), 417-425.
- Garcia, M., D. Riaño, E. Chuvieco, J. Salas & F. M. Danson (2011). Multispectral and LiDAR Data Fusion for Fuel Type Mapping Using Support Vector Machine and Decision Rules. *Remote Sensing of Environment*, 115, 1369-1379.

- Gornish, E. S. & T. E. Miller (2010). Effects of Storm Frequency on Dune Vegetation. *Global Change Biology*, 16, 2668-2675.
- Hesp, P. (2002). Foredunes and Blowouts: Initiation, Geomorphology and Dynamics. *Geomorphology*, 48, 245-268.
- Hesp, P. (2013). Conceptual Models of the Evolution of Transgressive Dune Field Systems. *Geomorphology*, 199, 138–149.
- Hosier, P. & W. Cleary (1977). Cyclic Geomorphic Patterns of Washover on a Barrier Island in Southeastern North Carolina. *Environmental Geology*, 2, 23-31.
- Houser, C., C. Hapke & S. Hamilton (2008). Controls on Coastal Dune Morphology, Shoreline Erosion and Barrier Island Response to Extreme Storms. *Geomorphology*, 100, 223-240.
- Houser, C. & S. Hamilton (2009). Sensitivity of Post-Hurricane Beach and Dune Recovery to Event Frequency. *Earth Surface Processes and Landforms*, 34, 613-628.
- Houser, C. (2012). Feedback between Ridge and Swale Bathymetry and Barrier Island Storm Response and Transgression. *Geomorphology*, 173, 1-16.
- Hugenholtz, C. & S. Wolfe (2005a). Biogeomorphic Model of Dune Field Activation and Stabilization on the Northern Great Plains. *Geomorphology*, 70, 53-70.
- Hugenholtz, C. & S. Wolfe (2005b). Recent Stabilization of Active Sand Dunes on the Canadian Prairies and Relation to Recent Climate Variations. *Geomorphology*, 68, 131-147.
- Jensen, J. R. (2005). *Introductory Digital Image Processing: A Remote Sensing Perspective*: Pearson Prentice Hall. Upper Saddle River, New Jersey.
- Klimes, L., J. Klimešová & J. Osbornova (1993). Regeneration Capacity and Carbohydrate Reserves in a Clonal Plant *Rumex Alpinus*: Effect of Burial. *Vegetation*, 109, 153-160.
- Leadon, M. E. (1999). Beach, Dune and Offshore Profile Response to a Severe Storm Event. Paper Presented at the Coastal Sediments (1999) Hauppauge, New York, United States.
- Li, J, J. Wan, Y. Lu, J. Chen, & Y. Fu. (2013). A New Object-Oriented Approach towards GIS Seamless Spatio-Temporal Data Model Construction. *Pervasive Computing and the Networked World*: Springer, Berlin Heidelberg.
- Matias, A., Ó. Ferreira, A. Vila-Concejo, T. Garcia & J. A. Dias (2008). Classification of Washover Dynamics in Barrier Islands. *Geomorphology*, 97, 655-674.

- Maun, M. A. (1996). The Effects of Burial by Sand on Survival and Growth of *Calamovilfa longifolia*. *Ecoscience. Sainte-Foy*, 3, 93-100.
- Maun, M. A. (1998). Adaptations of Plants to Burial in Coastal Sand Dunes. *Canadian Journal of Botany*, 76, 713-738.
- Maun, M. A. (2009). *The Biology of Coastal Sand Dunes*: Oxford University Press, New York.
- Maze, K. & R. Whalley (1992). Effects of salt spray and sand burial on *Spinifex sericeus* R. Br. *Australian Journal of Ecology*, 17, 9-19.
- McCall, R., J. Van Thiel de Vries, N. Plant, A. Van Dongeren, J. Roelvink, D. Thompson & A. Reniers (2010). Two-Dimensional Time Dependent Hurricane Overwash and Erosion Modeling at Santa Rosa Island. *Coastal Engineering*, 57, 668-683.
- Miller, D. L., M. Thetford & L. Yager (2001). Evaluation of Sand Fence and Vegetation for Dune Building following overwash by Hurricane Opal on Santa Rosa Island, Florida. *Journal of Coastal Research*, 936-948.
- Miller, T. E., E. S. Gornish & H. L. Buckley (2010). Climate and Coastal Dune Vegetation: Disturbance, Recovery, and Succession. *Plant Ecology*, 206, 97-104.
- Morton, R. A., J. G. Paine & J. C. Gibeaut (1994). Stages and Durations of Post-Storm Beach Recovery, Southeastern Texas Coast, USA. *Journal of Coastal Research*, 884-908.
- Mountrakis, G., J. Im & C. Ogole (2011). Support Vector Machines in Remote Sensing: A Review. *ISPRS Journal of Photogrammetry and Remote Sensing*, 66, 247-259.
- Myint, S. W., P. Gober, A. Brazel, S. Grossman-Clarke & Q. Weng (2011). Per-Pixel vs. Object-Based Classification of Urban Land Cover Extraction Using High Spatial Resolution Imagery. *Remote Sensing of Environment*, 115, 1145-1161.
- Otvos, E. G. (1982). Santa Rosa Island, Florida Panhandle, Origins of a Composite Barrier Island. *Southeastern Geology*, 23, 15-23.
- Partridge, T. (1992). Vegetation Recovery Following Sand Mining on Coastal Dunes at Kaitorete Spit, Canterbury, New Zealand. *Biological Conservation*, 61, 59-71.
- Randall, R. E. (1970). Vegetation and Environment on the Barbados Coast. *The Journal of Ecology*, 155-172.
- Richards, F. (1959). A Flexible Growth Function for Empirical Use. *Journal of Experimental Botany*, 10, 290-301.

- Safavian, S. R. & D. Landgrebe (1991). A Survey of Decision Tree Classifier Methodology. *IEEE Transactions on Systems, Man and Cybernetics*, 21, 660-674.
- Sallenger Jr, A. H. (2000). Storm Impact Scale for Barrier Islands. *Journal of Coastal Research*, 890-895.
- Snyder, R. & C. Boss (2002). Recovery and Stability in Barrier Island Plant Communities. *Journal of Coastal Research*, 530-536.
- Stallins, J. A. & A. J. Parker (2003). The Influence of Complex Systems Interactions on Barrier Island Dune Vegetation Pattern and Process. *Annals of the Association of American Geographers*, 93, 13-29.
- Stockdon, H. F., Holman, R. A., Howd, P. A., & Sallenger Jr, A. H. (2006). Empirical Parameterization of Setup, Swash, and Runup. *Coastal Engineering*, 53(7), 573-588.
- Stone, G. W., Stapor Jr, Frank W, May, James P, & Morgan, James P. (1992). Multiple Sediment Sources and a Cellular, Non-Integrated, Longshore Drift System: Northwest Florida and Southeast Alabama Coast, USA. *Marine Geology*, 105(1), 141-154.
- Stone, G. W., & Jr, Frank W. Stapor. (1996). A Nearshore Sediment Transport Model for the Northeast Gulf of Mexico Coast, U.S.A. *Journal of Coastal Research*, 12(3), 786-793.
- Stone, G. W., B. Liu, D. A. Pepper & P. Wang (2004). The Importance of Extratropical and Tropical Cyclones on the Short-Term Evolution of Barrier Islands along the Northern Gulf of Mexico, USA. *Marine Geology*, 210, 63-78.
- Tsoularis, A. & J. Wallace (2002). Analysis of logistic growth models. *Mathematical Biosciences*, 179, 21-55.
- Verhulst, P.-F. (1838). Notice sur la loi que la Population suit dans son Accroissement. *Correspondance Mathématique et Physique Publiée par A. Quetelet*, 10, 113-121.
- Webster, P. J., G. J. Holland, J. A. Curry & H.-R. Chang (2005). Changes in Tropical Cyclone Number, Duration, and Intensity in a Warming Environment. *Science*, 309, 1844-1846.
- Wolner, C. W. V., L. J. Moore, D. R. Young, S. T. Brantley, S. N. Bissett, and R. A. McBride (2013). Ecomorphodynamic Feedbacks and Barrier Island Response to Disturbance: Insights from the Virginia Barrier Islands, Mid-Atlantic Bight, USA. *Geomorphology*, 199(0), 115-128.

Zhang, J. & M. Maun (1990). Sand Burial Effects on Seed Germination, Seedling Emergence and Establishment of *Panicum Virgatum*. *Ecography*, 13, 56-61.

Zhang, J. & M. Maun (1992). Effects of Burial in Sand on the Growth and Reproduction of *Cakile Edentula*. *Ecography*, 15, 296-302.